Design, Synthesis, and Photodynamics of Light-Harvesting Arrays Comprised of a Porphyrin and One, Two, or Eight Boron-Dipyrrin Accessory Pigments

Feirong Li,[†] Sung Ik Yang,[‡] Yangzhen Ciringh,[†] Jyoti Seth,[§] Charles H. Martin, III,[⊥] Deepak L. Singh,[⊥] Dongho Kim,[‡,||] Robert R. Birge,*[,⊥] David F. Bocian,*[,§] Dewey Holten,*[,‡] and Jonathan S. Lindsey*[,†]

Contribution from the Departments of Chemistry, North Carolina State University, Raleigh, North Carolina 27695-8204, Washington University, St. Louis, Missouri 63130-4899, University of California, Riverside, California 92521-0403, and Syracuse University, 111 College Place, Syracuse, New York 13244-4100

Received April 9, 1998

Abstract: Light-harvesting arrays containing one, two, or eight boron-dipyrrin (BDPY) pigments and one porphyrin (free base or Zn chelate) have been synthesized using a modular building block approach. The reaction of pyrrole and 4-(BDPY)benzaldehyde or 3,5-bis(BDPY)benzaldehyde, prepared by Pd-mediated ethynylation with the corresponding iodo-benzaldehydes, affords the desired BDPY-porphyrin array in yields of 10−58%. The arrays are soluble in organic solvents and have been characterized by static and time-resolved absorption and fluorescence spectroscopy. The blue-green BDPY absorption complements spectral coverage of the porphyrin chromophores and rivals the intensity of the porphyrin Soret band when eight BDPY accessory pigments are present. Efficient energy transfer from the BDPY pigment(s) to the porphyrin (free base or Zn-chelate) is observed in arrays containing one or two (>90%) or eight (>85%) accessory pigments per porphyrin. Biphasic excited-state decay behavior is exhibited by the BDPY pigments in isolated form and in the arrays. The time constants are ∼15 and ∼500 ps in the reference compounds (both reflecting deactivation to the ground state) and ∼2 and ∼20 ps in the arrays (both primarily reflecting energy transfer to the porphyrin). The longer-lived kinetic component comprises ∼70% of the decay in each case. Ab initio calculations suggest that the two kinetic components are associated with two energetically accessible excited-state conformers involving the boron-dipyrrin unit and the 5-aryl ring (which is integral to the linker in the arrays). The calculations and experimental results indicate that the two excited-state conformers differ from one another in structure (the planarity of the boron-dipyrrin unit and its orientation with respect to the 5-aryl ring), electronic composition (especially the electron density on the 5-aryl group of the boron-dipyrrin unit), radiative and nonradiative coupling to the ground state, and the rate of energy transfer to the porphyrin constituent in the arrays. The high energy-transfer efficiencies together with favorable light-absorption and chemical properties exhibited by the boron-dipyrrin pigments make them amenable for use in porphyrin-based arrays for molecular photonics applications.

Introduction

Natural photosynthetic antenna complexes absorb light and funnel energy to the reaction centers.[1] Antenna complexes generally are heterogeneous assemblies of (bacterio)chlorophylls and accessory pigments embedded in protein matrices. The (bacterio)chlorophylls absorb strongly in the blue and red regions of the solar spectrum but are relatively transparent in the green region. Accessory pigments, such as carotenoids and bilins, absorb green light and transfer the harvested energy to the (bacterio)chlorophyll pigments. Naturally occurring antenna complexes serve as paradigms for the design of a variety of molecular photonic devices based on light-driven energy transfer, including artificial light-harvesting models, prototypes of molecular-scale information processing devices, and molecular-based sensors.

The development of efficient molecular photonic devices that utilize energy transfer presents interwoven design and synthesis challenges. The design challenges include selecting the individual pigments as well as planning the overall three-dimensional architecture. Issues relating to the selection of the pigments include the electronic structure (orbital energy spacing and ordering, electron-density distributions),[2] photophysical properties (absorption wavelengths and intensities, excited-state lifetimes),[3,4] and compatibility with the methods of synthesis

[†] North Carolina State University.
[‡] Washington University.
[§] University of California.
[⊥] Syracuse University.
[||] Permanent address: Spectroscopy Lab, Korea Research Institute of Standards and Science, P.O. Box 102, Yusong, Taejon 305-600, Korea.

(1) (a) Larkum, A. W. D.; Barrett, J. *Adv. Bot. Res.* **1983**, *10*, 1−219. (b) *Photosynthetic Light-Harvesting Systems*; Scheer, H., Siegried, S., Eds.; W. de Gruyter: Berlin 1988. (c) Mauzerall, D. C.; Greenbaum, N. L. *Biochim. Biophys. Acta* **1989**, *974*, 119−140. (d) Hunter, C. N.; van Grondelle, R.; Olsen, J. D. *Trends Biochem. Sci.* **1989**, *14*, 72−76. (e) McDermott, G.; Prince, S. M.; Freer, A. A.; Hawethornthwaite-Lawless, A. M.; Papiz, M. Z.; Cogdell, R. J.; Isaacs, N. W. *Nature* **1995**, *374*, 517−521. (f) Karrasch, S.; Bullough, P. A.; Ghosh, R. *EMBO J.* **1995**, *14*, 631−638.

(2) Strachan, J. P.; Gentemann, S.; Seth, J.; Kalsbeck, W. A.; Lindsey, J. S.; Holten, D.; Bocian, D. F. *J. Am. Chem. Soc.* **1997**, *119*, 11191−11201.

(3) Li, F.; Gentemann, S.; Kalsbeck, W. A.; Seth, J.; Lindsey, J. S.; Holten, D.; Bocian, D. F. *J. Mater. Chem.* **1997**, *7*, 1245−1262.

S0002-7863(98)01204-9 CCC: $15.00
Published on Web 09/19/1998

and purification. Issues relating to the overall architecture include chromophore substituents, linker types, pigment connection sites,[2] and interpigment distances and orientations. Collectively, these factors dictate the spectral coverage and light-absorption efficiency; the rates, efficiencies, and mechanisms of energy transfer (through-bond and/or through-space);[2,3,5−8] the direction of energy flow;[9] and the solubility (for chemical processing[10]). The synthetic challenge is to realize the design objective. Synthesis issues include preparing the individual pigments, joining the pigments using selective coupling methods, and purifying the resulting molecular photonic device.

Synthetic porphyrins have been frequently employed as light-absorbing and energy-transfer components of molecular devices. Porphyrins absorb strongly in the blue and weakly in the green region, mimicking the absorption properties of (bacterio)-chlorophyll pigments, though the former differ from the latter in absorbing only weakly in the red. However, porphyrins are more accessible synthetically than are (bacterio)chlorins. Numerous compounds have been prepared to investigate energy transfer between covalently linked porphyrins,[11] from one accessory pigment (anthracenyl-polyenes,[12] anthracenyl-polyynes,[13] boron-dipyrrin dyes,[14] carbocyanines,[15] carotenoids,[16] and polyynes[17]) to a porphyrin, or from four ruthenium coordination complexes to a porphyrin.[18]

A desirable architecture for efficient light-harvesting employs large numbers of accessory pigments that absorb light and transfer the energy directly to the acceptor.[9] We have initiated studies of boron-dipyrrin dyes as accessory pigments in porphyrin-containing arrays because these chromophores have a number of favorable properties. These characteristics include sharp (fwhm $\sim$ 25 nm) and moderately strong (ϵ = 40 000−100 000 $M^{-1}cm^{-1}$) absorption near 500 nm, long excited-state lifetimes ($\sim$5 ns for boron-dipyrrin dyes studied previously[19]), good solubility in organic solvents, and amenability toward chromatography on silica and alumina. The blue-green absorption of the boron-dipyrrin pigments (1) enables the pigment to enhance the absorption properties of associated arrays for light-harvesting applications and (2) facilitates relatively selective excitation of the pigment in the presence of free base or metalloporphyrins for applications in molecular photonic devices. Boron-dipyrrin dyes bearing pyrrole substituents, but lacking substituents at the methine (5-) position, were first prepared by Treibs and Kreuzer in 1968,[20] and have been widely used as fluorescent probes (Chart 1).[21] We recently developed a facile route to boron-dipyrrin dyes bearing substituents at the 5-position[22] that facilitates incorporation of these accessory pigments into porphyrin-containing molecular photonic wires[14a] and optoelectronic gates.[14b]

Chart 1. Boron-Dipyrrin Dyes

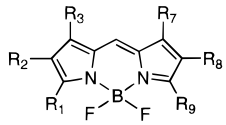

5−unsubstituted dyes

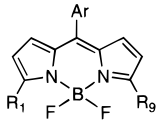

5-aryl substituted dyes

In this paper, we describe the synthesis and detailed photophysical characterization of arrays comprised of a porphyrin and one, two, or eight boron-dipyrrin pigments. The synthetic approach capitalizes on a building block strategy that has afforded light-harvesting arrays and molecular photonic devices comprised of metalloporphyrins and free base (Fb) porphyrins joined via *p,p′*-diarylethyne linkers.[11,23] In these latter multiporphyrin arrays, energy transfer was found to occur predominantly via a linker-mediated through-bond (TB) process rather than a through-space (TS) mechanism.[2,3,5−8] The photophysical studies of the boron-dipyrrin−porphyrin arrays studied herein elucidate a variety of fundamental properties of these light-harvesting architectures, including (1) the excited-state properties of boron-dipyrrin pigments, (2) the rate, efficiency, and mechanism of energy transfer from such an accessory pigment to a porphyrin, (3) the differences in the rates and efficiencies of energy transfer for *p,p′*-substituted versus *p,m′*-substituted diarylethyne linkers, and (4) the changes in the photophysical properties of the arrays as the number of pigments appended to one porphyrin is increased from one to eight. The synthetic and photophysical studies are augmented by theoretical calculations concerning the excited-state properties of the boron-dipyrrin pigments.

Results

Synthesis of Light-Harvesting Arrays. (1) Synthetic Strategy. In our modular building block approach for synthesizing multiporphyrin light-harvesting arrays and related molecular devices,[3,8,10,11,14,23] an aryl aldehyde bearing ethyne or iodo groups is reacted with pyrrole or a dipyrromethane for conversion to the porphyrin building block. Arrays are then formed by joining the porphyrin building blocks (each in a defined metalation state) via a Pd-mediated coupling method.[24] To cluster up to eight boron-dipyrrin dyes around the porphyrin,

(4) Yang, S. I.; Seth, J.; Strachan, J. P.; Gentemann, S.; Kim, D.; Holten, D.; Lindsey, J. S.; Bocian, D. F. *J. Porphyrins Phthalocyanines*, in press.
(5) Seth, J.; Palaniappan, V.; Johnson, T. E.; Prathapan, S.; Lindsey, J. S.; Bocian, D. F. *J. Am. Chem. Soc.* **1994**, *116*, 10578−10592.
(6) Hsiao, J.-S.; Krueger, B. P.; Wagner, R. W.; Delaney, J. K.; Mauzerall, D. C.; Fleming, G. R.; Lindsey, J. S.; Bocian, D. F.; Donohoe, R. J. *J. Am. Chem. Soc.* **1996**, *118*, 11181−11193.
(7) Seth, J.; Palaniappan, V.; Wagner, R. W.; Johnson, T. E.; Lindsey, J. S.; Bocian, D. F. *J. Am. Chem. Soc.* **1996**, *118*, 11194−11207.
(8) Strachan, J. P.; Gentemann, S.; Seth, J.; Kalsbeck, W. A.; Lindsey, J. S.; Holten, D.; Bocian, D. F. *Inorg. Chem.* **1998**, *37*, 1191−1201.
(9) Van Patten, P. G.; Shreve, A. P.; Lindsey, J. S.; Donohoe, R. J. *J. Phys. Chem. B* **1998**, *102*, 4209−4216.
(10) Lindsey, J. S.; Prathapan, S.; Johnson, T. E.; Wagner, R. W. *Tetrahedron* **1994**, *50*, 8941−8968.
(11) Wagner, R. W.; Johnson, T. E.; Lindsey, J. S. *J. Am. Chem. Soc.* **1996**, *118*, 11166−11180.
(12) (a) Effenberger, F.; Schlosser, H.; Bauerle, P.; Maier, S.; Port, H.; Wolf, H. C. *Angew. Chem., Int. Ed. Engl.* **1988**, *27*, 281−284. (b) Bonfantini, E. E.; Officer, D. L. *J. Chem. Soc., Chem. Commun.* **1994**, 1445−1446. (c) Wurthner, F.; Vollmer, M. S.; Effenberger, F.; Emele, P.; Meyer, D. U.; Port, H.; Wolf, H. C. *J. Am. Chem. Soc.* **1995**, *117*, 8090−8099.
(13) Kawabata, S.; Yamazaki, I.; Nishimura, Y. *Bull. Chem. Soc. Jpn.* **1997**, *70*, 1125−1133.
(14) (a) Wagner, R. W.; Lindsey, J. S. *J. Am. Chem. Soc.* **1994**, *116*, 9759−9760. (b) Wagner, R. W.; Lindsey, J. S.; Seth, J.; Palaniappan, V.; Bocian, D. F. *J. Am. Chem. Soc.* **1996**, *118*, 3996−3997.
(15) Lindsey, J. S.; Brown, P. A.; Siesel, D. A. *Tetrahedron* **1989**, *45*, 4845−4866.
(16) (a) Gust, D.; Moore, T. A.; Moore, A. L.; Devadoss, C.; Liddell, P. A.; Hermant, R.; Nieman, R. A.; Demanche, L. J.; DeGraziano, J. M.; Gouni, I. *J. Am. Chem. Soc.* **1992**, *114*, 3590−3603. (b) Moore, T. A.; Gust, D.; Moore, A. L. *Pure Appl. Chem.* **1994**, *66*, 1033−1040.
(17) Maruyama, K.; Kawabata, S. *Bull. Chem. Soc. Jpn.* **1989**, *62*, 3498−3507.
(18) Collin, J.-P.; Harriman, A.; Heitz, V.; Odobel, F.; Sauvage, J.-P. *J. Am. Chem. Soc.* **1994**, *116*, 5679−5690.
(19) Karolin, J.; Johansson, L. B.-A.; Strandberg, L.; Ny, T. *J. Am. Chem. Soc.* **1994**, *116*, 7801−7806.
(20) Treibs, A.; Kreuzer, F. H. *Liebigs Ann. Chem.* **1968**, *718*, 208−223.
(21) (a) Wories, H. J.; Koek, J. H.; Lodder, G.; Lugtenburg, J.; Fokkens, R.; Driessen, O.; Mohn, G. R. *Recl. Trav. Chim. Pays-Bas* **1985**, *104*, 288−291. (b) Haugland, R. P.; Kang, H. C. U.S. Patent 4, 774, 339, 1988. (c) Molecular Probes, Inc., Eugene, OR.
(22) Wagner, R. W.; Lindsey, J. S. *Pure Appl. Chem.* **1996**, *68*, 1373−1380.
(23) Lindsey, J. S. In *Modular Chemistry*; Michl, J., Ed.; NATO ASI Series C: Mathematical and Physical Sciences 499; Kluwer Academic Publishers: Dordrecht, 1997; pp 517−528.

Chart 2. Boron-Dipyrrin Compounds Studied Here[a]

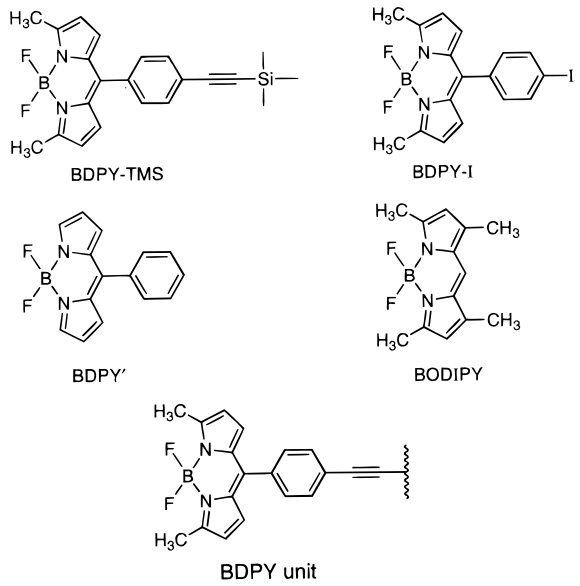

[a] The BDPY-TMS compound was used as the reference for photophysical measurements on the arrays.

we have developed methodology to utilize the *meta*-positions of the *meso*-aryl rings on the porphyrin. Our approach here reverses the "porphyrin-formation-first, coupling-second" strategy and allows the preparation of arrays consisting of one porphyrin and one, two, or eight of the boron-dipyrrin structural units (hereafter abbreviated BDPY) depicted in Chart 2. In this approach, the BDPY unit is incorporated into the aryl aldehyde unit at the 4- or 3,5-positions via the Pd-mediated coupling reaction. Then the BDPY-substituted aldehyde is condensed with pyrrole to afford the desired BDPY-substituted porphyrin. This approach relies on the robustness of porphyrin formation to arrange up to eight boron-dipyrrin pigments around the porphyrin, rather than a succession of Pd-mediated coupling reactions with a pigment and a highly substituted porphyrin.

(2) Benzaldehydes Substituted with Boron-Dipyrrin Pigments. 5-Substituted boron-dipyrrin dyes (Chart 2) are readily accessible by a one-flask synthesis of 5-substituted dipyrromethanes from an aldehyde and pyrrole, followed by a one-flask process of oxidation and boron complexation.[22] Although the overall yield is only ~10%, the synthesis is robust and affords dyes bearing functional groups (iodo, ethyne) at the 5-positions for further elaboration. Each of these dyes lacks substituents at the β-pyrrole positions. The commercially available boron-dipyrrin dyes generally have β-pyrrole substituents but lack substituents at the 5-position, as shown for BODIPY in Chart 2.

The introduction of a BDPY unit at the 4-position of an aryl aldehyde (Scheme 1) relies on the Pd-mediated coupling of an aryl ethyne and an aryl iodide.[25] Samples of 4-ethynylbenzaldehyde[26] (47 mM) and BDPY-I[14,22] (40 mM) were coupled in

Scheme 1. Formation of 4-(BDPY)benzaldehyde (**1**)

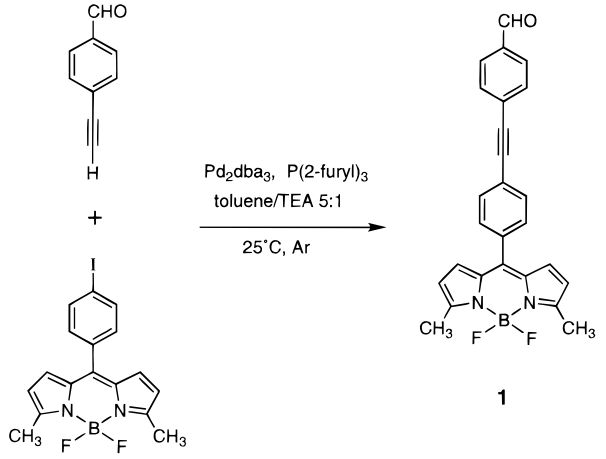

toluene/triethylamine (TEA) (5:1) in the presence of tris(dibenzylideneacetone)dipalladium(0) (Pd_2dba_3, 0.5 mol %/I) and tri(2-furyl)phosphine [$P(2\text{-furyl})_3$, 400 mol %/Pd] under argon at room temperature. After 20 h, column chromatography of the reaction mixture afforded 4-(BDPY)benzaldehyde (**1**) in 98% yield.

The synthetic routes for preparing 3,5-bis(BDPY)benzaldehyde are shown in Scheme 2. Aminoester **2** at one time was commercially available but has been discontinued, and aldehydes **5** and **6** have been prepared previously starting with 1,3,5-tribromobenzene.[27] Here we include a complete route to obtain the desired 3,5-bis(BDPY)benzaldehyde via the key intermediate 3,5-diiodobenzaldehyde (**4**). Treatment of methyl 4-aminobenzoate with excess ICl afforded **2** in 60% yield, while Fischer esterification of 4-amino-3,5-diiodobenzoic acid gave **2** in quantitative yield. Deamination of aminoester **2** with isopentyl nitrite in THF[28] afforded **3** (71% yield), which upon reduction with DIBALH and oxidation of the resulting benzyl alcohol with PCC afforded **4** in 84% yield. Pd-mediated ethynylation of aldehyde **4** afforded **5** (46% yield), which upon desilylation afforded 3,5-diethynylbenzaldehyde (**6**). This diethyne has been reported to be unstable,[27] but at the half-gram scale in our hands **6** was quite stable and was readily chromatographed. Pd-mediated coupling of **6** with BDPY-I afforded the 3,5-bis(BDPY)benzaldehyde (**7**) in 81% yield.

(3) Light-Harvesting Arrays. The porphyrin containing one BDPY unit at the 4-position of the *meso*-aryl group was prepared by a mixed aldehyde condensation in the room-temperature porphyrin reaction (Scheme 3).[10] Condensation of pyrrole (10^{-2} M), mesitaldehyde, and aldehyde **1** (4:3:1 ratio) in $CHCl_3$ with $BF_3{\cdot}O(Et)_2$ (6.6 mM) followed by oxidation with DDQ afforded five porphyrin bands upon TLC analysis. Column chromatography afforded the monosubstituted Fb porphyrin $(BDPY)_1$-*p*-Fb (**8**) in 21% yield and the *cis*-substituted complex $(BDPY)_2$-*p*-Fb (**9**) in 10% yield. Treatment of Fb porphyrin **8** with methanolic $Zn(OAc)_2$ afforded the zinc chelate $(BDPY)_2$-*p*-Zn (**Zn-8**) in quantitative yield.

Two BDPY units can be introduced on the same porphyrin *meso*-aryl ring, as shown in Scheme 4. The mixed aldehyde condensation of pyrrole (10^{-2} M), mesitaldehyde, and aldehyde **7** (4:3:1 ratio) in $CHCl_3$ with 6.6 mM $BF_3{\cdot}O(Et)_2$ afforded a mixture of six porphyrins. The bis-substituted complex $(BDPY)_2$-

(24) Wagner, R. W.; Johnson, T. E.; Li, F.; Lindsey, J. S. *J. Org. Chem.* **1995**, *60*, 5266−5273.

(25) The Pd-coupling methods used in this work have not been optimized and differ in several ways from those optimized for porphyrin couplings:[24] (1) Tri(2-furyl)phosphine was generally employed rather than triphenylarsine ($AsPh_3$) (the latter is superior in porphyrin couplings). (2) The greater solubility of the aryl aldehydes compared with porphyrins in the reaction solvent (toluene/triethylamine 5:1) permits nearly 10-fold higher reaction concentrations (~40 mM). (3) Lesser amounts of Pd catalyst (0.5−2 mol %) and ligand were employed.

(26) Austin, W. B.; Bilow, N.; Kelleghan, W. J.; Lau, K. S. Y. *J. Org. Chem.* **1981**, *46*, 2280−2286.

(27) (a) Saf, R.; Swoboda, P.; Hummel, K. *J. Heterocycl. Chem.* **1993**, 425−428. (b) Chen, L. S.; Chen, G. J.; Tamborski, C. *J. Organomet. Chem.* **1980**, *215*, 281−291.

(28) Cadogan, J. I. G.; Molina, G. A. *J. Chem. Soc., Perkin Trans. 1* **1973**, 541−542.

Scheme 2. Synthesis of Versatile Benzaldehydes **4** and **6** and the 3,5-Bis(BDPY)benzaldehyde (**7**)

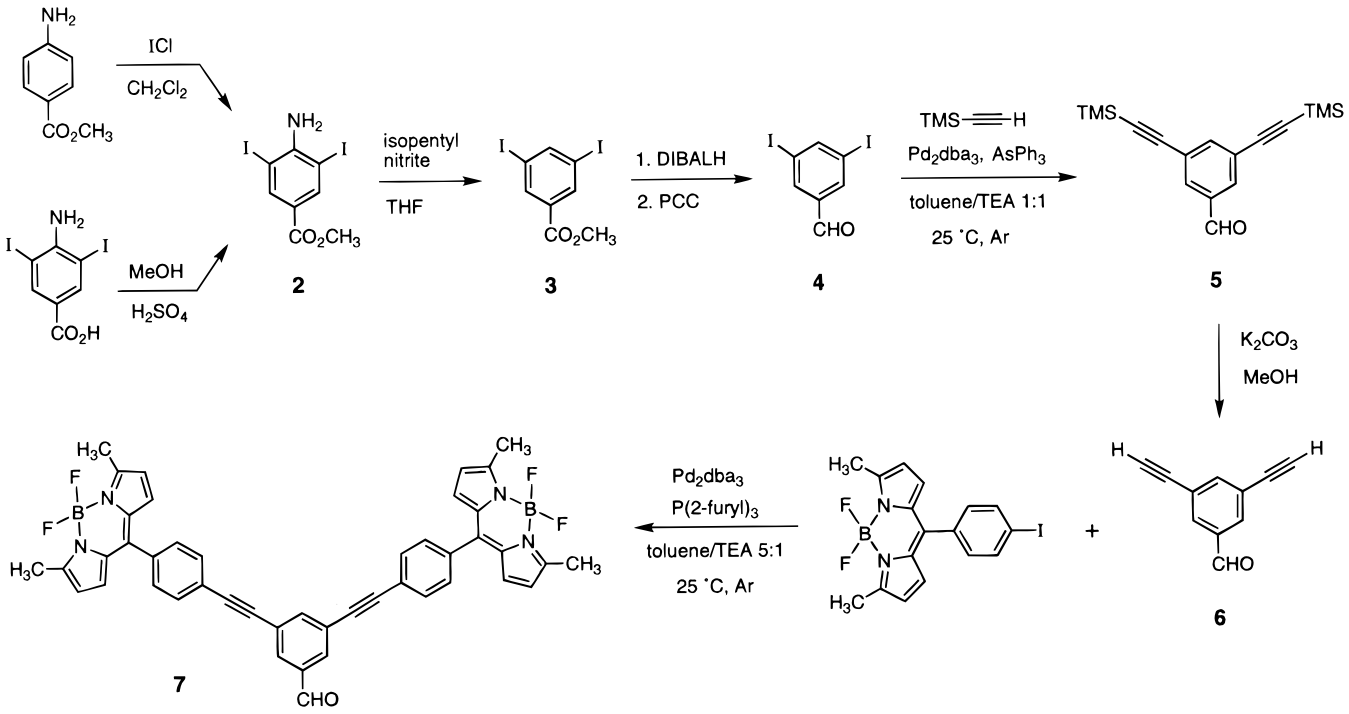

Scheme 3. Mixed-Aldehyde Condensation Forming *para*-Substituted (BDPY)porphyrins

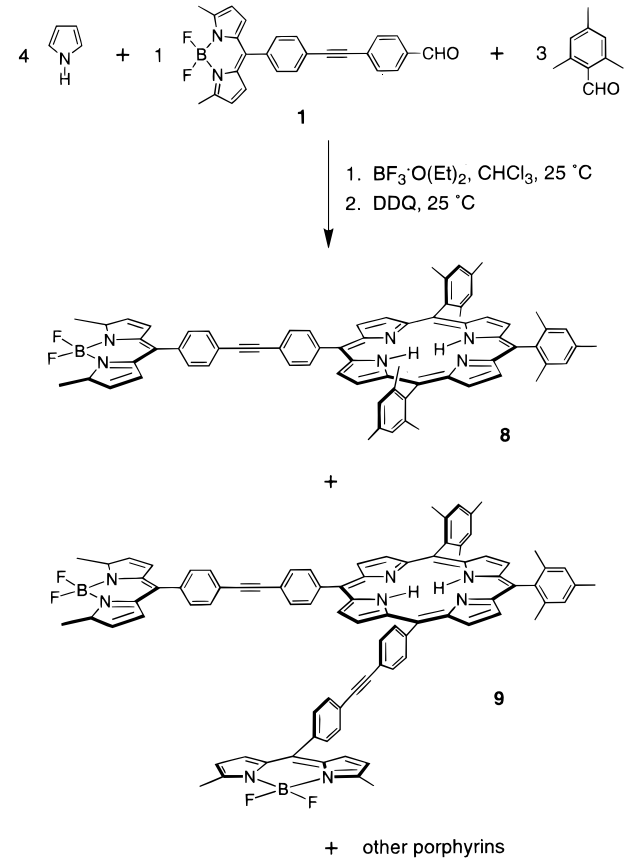

Scheme 4. Mixed-Aldehyde Condensation Yielding the *meta*-Substituted (BDPY)$_2$porphyrin **10**

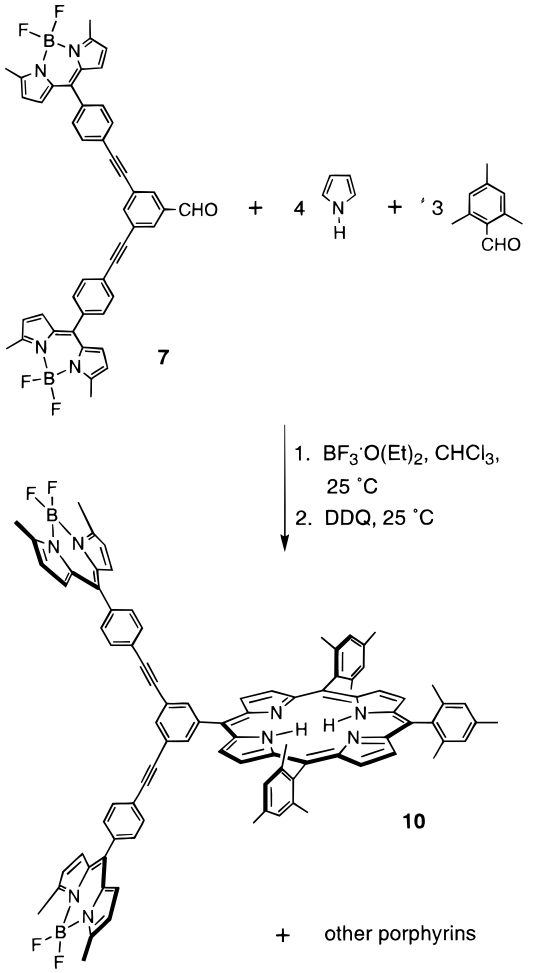

m-Fb (**10**) appeared as the most intense band via TLC analysis and was isolated in 19% yield following purification by two silica columns. During the course of this work, we found that concentrations of $BF_3{\cdot}O(Et)_2$ about 2 times that employed normally (3.3 mM) afford enhanced yields for the various BDPY-substituted aldehydes.

To prepare an array comprised of a cluster of BDPY units arranged around a porphyrin, we condensed 3,5-bis(BDPY)-

Scheme 5. One-Flask Synthesis of $(BDPY)_8$-*m*-Fb Porphyrin **11**

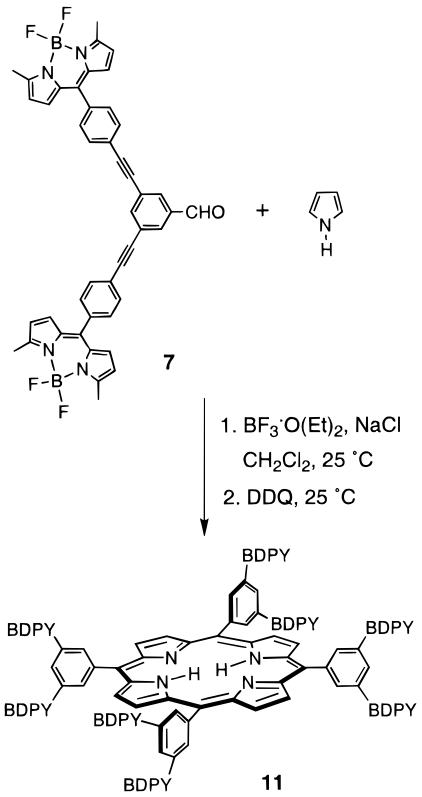

benzaldehyde (**7**) directly with pyrrole (Scheme 5). On a small scale in $CHCl_3$ using 10^{-2} M reactants, the yield of **11** determined spectroscopically increased with $BF_3{\cdot}O(Et)_2$ concentration to 12% (6.6 mM $BF_3{\cdot}O(Et)_2$), 24% (13.2 mM), and 50% (19.8 mM). Reactions performed with the addition of salt (1 mM $BF_3{\cdot}O(Et)_2$, CH_2Cl_2, and 1 or 2 equiv of NaCl), which we recently found to give improved yields with some aldehydes,[29] afforded a 50% yield. The latter reaction was scaled-up, affording the octa-substituted porphyrin $(BDPY)_8$-*m*-Fb (**11**) in 58% yield upon chromatography with an alternating sequence of adsorption and size-exclusion chromatography[24] columns. Treatment of **11** with methanolic $Zn(OAc)_2$ gave $(BDPY)_8$-*m*-Zn (**Zn-11**) in 96% yield. However, attempts to prepare the corresponding magnesium chelate using either the heterogeneous or homogeneous magnesium-insertion methods were unsuccessful.[30]

The CPK model of $(BDPY)_8$-*m*-Fb (**11**) is shown in Figure 1. The attachment of the linker at the *meta* position of the *meso*-aryl ring creates a three-dimensional architecture, with the BDPY units thrust away from the porphyrin. A range of molecular motion is possible in this architecture. (1) The 5-aryl boron-dipyrrin unit undergoes relatively free rotation about the cylindrically symmetric ethyne in the linker. (2) The 5-aryl group and the boron-dipyrrin unit undergo torsional motion about the aryl−dipyrrin single bond. (3) The *meso*-aryl group and the porphyrin undergo torsional motion about the *meso*-aryl−porphyrin single bond. (4) The entire *p,m′*-diarylethyne unit is expected to undergo substantial bending as was observed for *p,p′*-diarylethyne linkers.[31] Such torsional motions and free rotation about the ethyne are of little consequence in the BDPY-porphyrin systems with *p,p′*-diarylethyne linkers. However, in the *meta*-substituted BDPY-porphyrin systems, rotation of the *meso*-aryl unit pushes the neighboring BDPY units into close proximity. Indeed, rotation of adjacent *meso*-aryl units by ±30° from the normal with respect to the porphyrin plane allows contact of two adjacent BDPY pigments (that in turn are freely rotating about the ethyne linker).

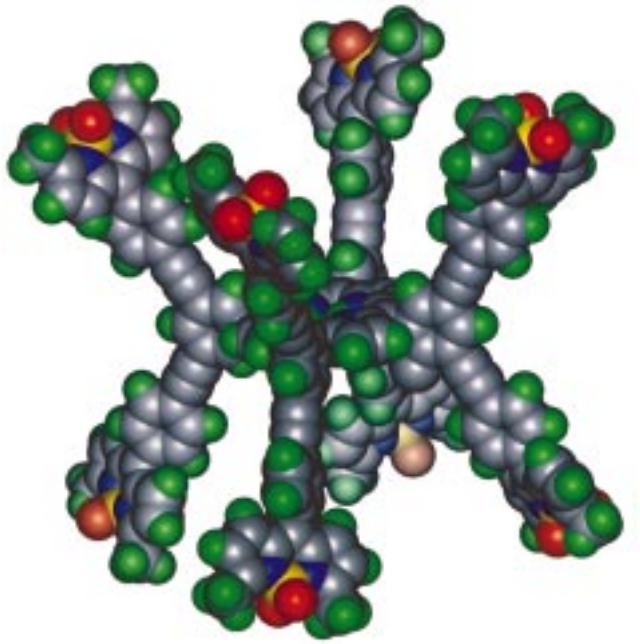

Figure 1. CPK model of $(BDPY)_8$-*m*-Fb. The boron-dipyrrin units are shown rotated 52° with respect to the 5-aryl substituent, and the *meso*-aryl units are shown in a perpendicular conformation with respect to the porphyrin plane. Rotation of adjacent *meso*-aryl units by ±30° from the normal with respect to the porphyrin plane causes contact of the pyrrolic units of the BDPY pigments.

Table 1. Half-Wave Potentials ($E_{1/2}$) for the BDPY-Containing Compounds[a]

	oxidation			reduction		
	BDPY	porphyrin		BDPY	porphyrin	
		$E_{1/2}(1)$	$E_{1/2}(2)$		$E_{1/2}(1)$	$E_{1/2}(2)$
BDPY′	1.14			−1.12		
$(BDPY)_1$-*p*-Fb	1.05	0.65	0.88	*b*	−0.88	−1.28
$(BDPY)_1$-*p*-Zn	1.00	0.40	0.73	*b*	−1.26	−1.75
$(BDPY)_2$-*p*-Fb	1.10	0.67	0.89	*b*	−0.88	−1.28
$(BDPY)_2$-*m*-Fb	1.10	0.67	0.89	*b*	−0.88	−1.28

[a] Obtained in acetonitrile containing 0.1 M TBAH. $E_{1/2}$ vs Ag/Ag^+; $E_{1/2}$ of $FeCp_2/FeCp_2^+$ = 0.03 V. Values are ±0.01V. [b] The reduction wave for the BDPY unit is obscured by the waves from the porphyrin, and the exact $E_{1/2}$ value is not certain (see text).

Chemical and Physical Properties of the Arrays and Precursors. (1) Purity, Solubility, and Stability. A high level of purity, solubility, and stability is essential for routine handling and spectroscopic analysis of the arrays. The purity of each array is estimated to be >98% (see Supporting Information). The arrays were soluble at 5−15 mM in CH_2Cl_2/hexanes 1:1, CH_2Cl_2, $CHCl_3$, $CDCl_3$, or toluene, a convenient concentration for chromatography and NMR analysis. Optical spectroscopic studies were performed at 1−200 μM in a wide range of solvents, including acetonitrile, dimethyl sulfoxide, 3-methylpentane, and mineral oil. The arrays were stable during routine handling on the benchtop.

(2) Redox Properties. The electrochemical data for the various compounds are summarized in Table 1. The $E_{1/2}$ values

(29) Li, F.; Yang, K.; Tyhonas, J. S.; MacCrum, K. A.; Lindsey, J. S. *Tetrahedron* **1997**, *53*, 12339−12360.

(30) (a) Lindsey, J. S.; Woodford, J. N. *Inorg. Chem.* **1995**, *34*, 1063−1069. (b) O'Shea, D. F.; Miller, M. A.; Matsueda, H.; Lindsey, J. S. *Inorg. Chem.* **1996**, *35*, 7325−7338.

(31) Bothner-By, A.; Dadok, J.; Johnson, T. E.; Lindsey, J. S. *J. Phys. Chem.* **1996**, *100*, 17551−17557.

Table 2. Absorption Properties of Arrays and Reference Compounds in Toluene at 298 K

compound	no. of BDPY pigments	λ_{max} (fwhm)	$\epsilon_{516\ nm}/\epsilon_{Soret}$ (%)	$\epsilon_{516\ nm(BDPY)}/\epsilon_{516\ nm(total)}$ (%)[a]	$\epsilon_{485\ nm(BDPY)}/\epsilon_{485\ nm(total)}$ (%)[a]
		Monomers			
BDPY-TMS	1	516 (25.0)	na[b]	100	100
FbTPP	0	419 (12.0), 514, 548, 592, 646	5.1	na	na
FbTMP	0	419 (12.5), 514, 544, 592, 650	5.0	na	na
ZnTPP	0	423 (11.5), 549, 588	0.9	na	na
		Arrays			
$(BDPY)_1$-*p*-Fb (**8**)	1	421 (13.0), 516 (23.0), 593, 650	19	68	83
$(BDPY)_1$-*p*-Zn (**Zn-8**)	1	423 (12.5), 516 (25.5), 550, 590	14	91	84
$(BDPY)_2$-*p*-Fb (**9**)	2	423 (14.0), 516 (23.5), 593, 650	34	81	91
$(BDPY)_2$-*m*-Fb (**10**)	2	422 (12.0), 516 (24.0), 592, 648	34	81	91
$(BDPY)_8$-*m*-Fb (**11**)	8	429 (12.5), 517 (27.5), 588, 648	84	94	97
$(BDPY)_8$-*m*-Zn (**Zn-11**)	8	433 (13.0), 517 (28.0), 590	91	99	98

[a] BDPY-TMS and FbTPP or ZnTPP were used as references for each array. [b] na, not applicable.

were obtained by square wave voltammetry (frequency = 10 Hz). The isolated chromophore BDPY′ (see Chart 2) exhibits one broad irreversible oxidation wave and one broad reversible reduction wave in the +1.3 to −2.0 V range. The redox potentials and behavior for BDPY′ are typical of those observed for other boron-dipyrrin dyes.[32] The oxidation behavior of the BDPY unit of the BDPY-porphyrin compounds is similar to that of BDPY′. The oxidation potential for the BDPY unit of the BDPY-porphyrins is somewhat lower than that of BDPY′ because the former compounds contain electron-donating methyl groups at the α-positions of the pyrrole rings, whereas the latter compound is unsubstituted (see Chart 2).[32] The reduction wave for the BDPY unit of the BDPY-porphyrins is obscured by waves for the Zn and Fb porphyrins. However, on the basis of the oxidation behavior of the BDPY unit, the reduction wave is expected to fall near −1.2 V. The porphyrin units of the BDPY-porphyrin compounds exhibit two reversible oxidation and two reversible reduction waves in the +1.3 to −2.0 V range. The redox potentials and behavior of the Zn and Fb porphyrins are typical of those observed for other tetraarylporphyrins.[33] In general, the redox characteristics of the BDPY-porphyrin arrays show no evidence for any appreciable interactions between the BDPY and porphyrin constituents.

(3) Absorption Spectra. The absorption spectra of the BDPY-porphyrin complexes and related reference compounds were measured in toluene at room temperature (Table 2). The Soret maxima (421−423 nm) of arrays containing one or two BDPY units are slightly (1−4 nm) red-shifted from those of the parent tetraphenyl- and tetramesitylporphyrins (ZnTPP, FbTPP, ZnTMP, and FbTMP). Significantly larger (10−14 nm) bathochromic shifts are found for $(BDPY)_8$-*m*-Fb (Figure 2) and $(BDPY)_8$-*m*-Zn. In the visible region, the two Q_x-bands of the Fb porphyrins (∼590 and ∼650 nm) and the two Q-bands of the Zn chelates (∼550 and ∼590 nm) exhibit relatively small (1−4 nm) shifts in peak positions in the arrays relative to the parent porphyrins. The two Q_y-bands of the Fb porphyrins (∼515 and ∼550 nm) are largely obscured by BDPY absorption, which is represented by the properties of the BDPY-TMS reference compound (λ_{max} = 516 nm, ϵ = 48 800 M^{-1} cm^{-1}, and fwhm ∼25 nm) (Chart 2).[22] The boron-dipyrrin pigment absorbs strongly in the blue-green, a region where the porphyrin absorbs weakly. The stronger absorption by the BDPY versus the porphyrin constituents in the blue-green region enables relatively selective excitation of the former. As the number of BDPY units increases from one to eight in the arrays, the relative absorption at 516 nm of the BDPY increases from 68 to 94% for the Fb porphyrin-containing arrays, and from 91 to 99% for the Zn porphyrin-containing arrays (Table 2). Similar ratios hold at 485 nm, where the BDPY has a shoulder and the porphyrin absorption is even weaker. In terms of spectral coverage, the strong absorption of BDPY accessory pigments enhances the light-harvesting capabilities of the arrays by complementing the porphyrin spectral characteristics. Indeed, the total blue-green absorption due to the BDPY pigments rivals that of the porphyrin Soret band in $(BDPY)_8$-*m*-Fb (Figure 2) and $(BDPY)_8$-*m*-Zn.

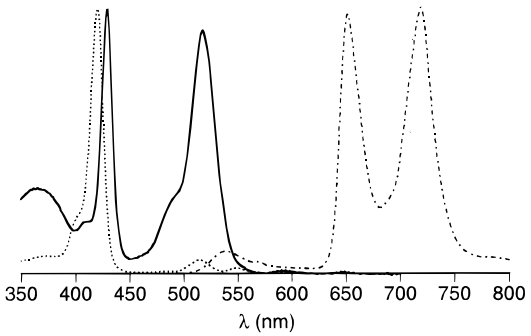

Figure 2. Overlay of the absorption spectrum of FbTPP (dashed line) with the absorption spectrum (solid line) and the fluorescence emission spectrum (dot−dashed line) of $(BDPY)_8$-*m*-Fb (**11**) obtained upon illumination at 485 nm (toluene, 298 K).

(4) Fluorescence Spectra and Quantum Yields. The fluorescence emission spectra of the BDPY-porphyrin arrays and appropriate reference compounds were recorded in toluene at room temperature. The fluorescence quantum yields are summarized in Table 3. For each of the Fb-porphyrin-containing arrays, excitation at the Soret maximum near 420 nm (where the absorption is due almost exclusively to the Fb porphyrin) gives typical Fb porphyrin emission with a quantum yield (0.11−0.14) comparable to that for FbTPP (0.11).[34] Illumination at 485 nm, where the BDPY pigment(s) absorb 83−97% of the light, produces emission predominantly from the Fb porphyrin with only a small amount of emission characteristic of the BDPY constituent (λ_{max} = 535 nm)[22] (Figure 2). Similar spectral features are observed upon excitation near 516 nm, where the BDPY constituents absorb 70−95% of the light. The diminished BDPY fluorescence yield, the unaltered Fb porphyrin emission, and the extensive emission from the Fb porphyrin upon illumination of the BDPY unit are consistent with a high yield of energy transfer from the BDPY to the Fb porphyrin. The Zn-porphyrin-containing arrays also

(32) Kollmannsberger, M.; Gareis, T.; Heinl, S.; Breu, J.; Daub, J. *Angew. Chem., Int. Ed. Engl.* **1997**, *36*, 1333−1335.

(33) Felton, R. H. In *The Porphyrins*; Dolphin, D., Ed.; Academic Press: New York, 1978; Vol. V, pp 53−126.

(34) Seybold, P. G.; Gouterman, M. *J. Mol. Spectrosc.* **1969**, *31*, 1−13.

Table 3. Photophysical Data for BDPY-Porphyrin Arrays and Reference Compounds[a]

compound	solvent	Φ_f(porph)[b]	τ(porph)[c] (ns)	Φ_f(BDPY)[d]	BDPY lifetimes[e] τ_a (ps)	χ_a	τ_b (ps)	χ_b
			Monomers					
FbTPP	toluene	0.11[f]	13.0 ± 0.6[g]					
FbTMP	toluene	0.10[g]	13.2 ± 0.6[g]					
ZnTPP	toluene	0.033[f]	2.0 ± 0.2[g]					
ZnTMP	toluene	0.031[g]	2.4 ± 0.3[g]					
BODIPY	toluene			0.51[h]	11 ± 1	0.22	5000 ± 30[i]	0.78
BDPY-I	toluene			0.18[j]	15 ± 3	0.28	1900 ± 300	0.72
BDPY′	toluene			0.053[k]	17 ± 2	0.45	440 ± 60	0.55
BDPY-TMS	Toluene			0.058[l]	15 ± 4	0.26	520 ± 50	0.74
	CH_3CN			0.029	23 ± 9	0.28	230 ± 50	0.72
	3-MePent				33 ± 8	0.24	650 ± 150	0.76
			Arrays					
$(BDPY)_1$-*p*-Fb (**8**)	toluene	0.12	10.2 ± 0.5	0.004	2.4 ± 0.4[m]	0.36	23 ± 2[m]	0.64
	CH_3CN	0.078	8.5 ± 0.4		1.7 ± 0.7	0.29	23 ± 2	0.71
	DMSO				1.3 ± 0.5	0.24	15 ± 1	0.76
	min oil				1.9 ± 0.6	0.21	28 ± 3	0.79
$(BDPY)_1$-*p*-Fb (**Zn-8**)	toluene	0.031	2.0 ± 0.2	0.002	1.8 ± 0.4	0.31	16 ± 1	0.69
	CH_3CN	0.003	0.034 ± 0.005[n]		0.4 ± 0.2	0.35	7.7 ± 0.4	0.65
$(BDPY)_2$-*p*-Fb (**9**)	toluene	0.14	9.9 ± 0.5	0.006	2.4 ± 0.5	0.45	25 ± 4	0.55
$(BDPY)_2$-*m*-Fb (**10**)	toluene	0.11	12.1 ± 0.6	0.005	1.8 ± 0.5	0.34	23 ± 2	0.66
$(BDPY)_8$-*m*-Fb (**11**)	toluene	0.13	11.2 ± 0.6	0.008	1.5 ± 0.4	0.55	15 ± 3	0.45
$(BDPY)_8$-*m*-Fb (**Zn-11**)	toluene	0.037		0.002	1.5 ± 0.3	0.45	15 ± 2	0.55

[a] Data were acquired at room temperature. Solvents: 3-MePent, 3-methylpentane; DMSO, dimethylsulfoxide; min oil, mineral oil. [b] The emission from Fb-porphyrin (λ_{exc} = 421−429 nm, where the Fb-porphyrin absorbs almost exclusively) was measured using two methods, and the average is reported. The first method involves measuring the emission intensity from 685 to 800 nm, where only the porphyrin emits, and inferring the total emission from 600 to 800 nm assuming the Fb-porphyrin in the array has the same emission spectral profile as FbTPP. In the second method, the emission from 500 to 550 nm (due solely to BDPY pigments) was used to infer the total BDPY emission from 500 to 800 nm (assuming the BDPY emission in the arrays has the same emission spectral profile as BDPY-TMS). The remaining emission from 500 to 800 nm was then attributed to the Fb-porphyrin. The latter method was also used to determine the emission from the Zn-porphyrin (λ_{exc} = 424 or 433 nm, where the Zn-porphyrin absorbs almost exclusively) over the region of 500−800 nm. [c] Unless indicated otherwise, the lifetime was determined by time-resolved fluorescence. [d] The emission from the BDPY pigments (λ_{exc} = 485 nm, where the fractional absorption of the BDPY pigments is listed in Table 2) was measured from 500 to 800 nm. The total emission from the BDPY was inferred by measurement of the emission intensity in the 500−550-nm region and assuming the BDPY in the array has the same emission spectral profile as in BDPY-TMS. [e] Unless indicated otherwise, measured by transient absorption spectroscopy exciting between 513 and 517 nm and probing the BDPY bleaching recovery at 515 nm. [f] From ref 34. [g] From ref 4. [h] In EtOH, values of 0.69 and 0.80 were determined here and in ref 19, respectively. [i] Measured by time-resolved fluorescence spectroscopy. The amplitudes of the two components were obtained from the transient absorption data by fixing the lifetime of the slow component of the decay of the 515-nm BDPY bleaching at 5 ns. [j] A value of 0.21 is reported in ref 22. [k] From ref 22. [l] Revises the value 0.078 reported in ref 22. [m] Components having similar time constants are also found in the rise of the Fb bleaching at 650 nm using 480-nm excitation. The latter components have lifetimes of 1.8 ± 0.7 and 30 ± 6 ps and approximately equal amplitudes. [n] Determined via transient absorption spectroscopy by decay of the Zn bleaching at 550 nm following excitation at 515 nm.

exhibited similar properties, indicating a high yield of energy transfer in each case.

The yield of energy transfer (Φ_{trans}) can be quantitated through use of static fluorescence spectra in three different ways: (1) determination of the extent of quenching of the BDPY fluorescence, (2) comparison of the yield of porphyrin emission upon illumination of matched samples (at λ_{exc}) of the porphyrin (λ_{exc} = 420 nm) and the BDPY-porphyrin (λ_{exc} = 516 nm), and (3) comparison of the absorption and fluorescence excitation spectra of the BDPY-porphyrin (normalized in the Soret band).[35] The BDPY fluorescence is quenched by 7−30-fold in the various arrays, implying energy-transfer yields of 90−96% for all the arrays except $(BDPY)_8$-*m*-Fb, for which a value of 86% is derived. The quantum yield of porphyrin emission determined using matched samples of FbTPP versus the BDPY-Fb-porphyrin indicates that the energy-transfer efficiency is 93−98% for the arrays containing one or two BDPYs per porphyrin and 75% for $(BDPY)_8$-*m*-Fb. The respective absorption and excitation spectra matched closely for all arrays with one or two BDPY units, indicating >96% yields of energy transfer. However, in the arrays with eight BDPY units, the BDPY excitation band reached only 80−83% of the absorption intensity, implying energy-transfer yields of 80−83%. Inspection of these results indicates that the values from the measurements for a given array are in good agreement, with the maximum and minimum values differing by no more than 13%. Therefore, an average value of Φ_{trans} from the static emission measurements for each array is given in Table 4. These results imply nearly quantitative energy transfer in the arrays with one or two BDPY units but slightly lower (80−90%) efficiency in the arrays with eight BDPY units.

(5) Time-Resolved Spectroscopy. (a) BDPY-Porphyrins in Toluene. To probe the dynamics of energy transfer and to obtain additional estimates for the energy-transfer yields, the excited-state lifetimes of the BDPY and porphyrin chromophores in the arrays and associated reference compounds were monitored using time-resolved absorption and fluorescence techniques. Figure 3 shows representative transient absorption data for $(BDPY)_1$-*p*-Fb in toluene. The 0.1-ps 513-nm excitation flashes predominantly pump the BDPY pigment. Thus, the spectrum at 0.6 ps is dominated by bleaching of the BDPY ground-state absorption band at 515 nm. There is no easily discernible sign of bleaching of the ground-state absorption bands of the Fb porphyrin in this early-time spectrum. As time proceeds, the BDPY bleaching diminishes, and bleaching in the ground state absorption bands of the Fb porphyrin concomitantly grows. This fact can be seen in the 94-ps spectrum, which clearly exhibits bleaching in the porphyrin $Q_y(1,0)$ and $Q_y(0,0)$ bands near 515 and 545 nm, as well as evidence for bleaching in the $Q_x(1,0)$ band at 590 nm (Figure 3, top panel). The

(35) Stryer, L.; Haugland, R. P. *Proc. Natl. Acad. Sci. U.S.A.* **1967**, *58*, 719−726.

Table 4. Energy-Transfer Rates and Efficiencies Determined by Transient Absorption and Static Emission Spectroscopy

		transient absorption[a]								
compound	solvent	$[k_{trans(R)}]^{-1}$ (ps)[b]	$[k_{trans(M)}]^{-1}$ (ps)[c]	$\phi_{trans(R)}$[d]	$\phi_{trans(M)}$[e]	$\chi_R\phi_{trans(R)}$	$\chi_M\phi_{trans(M)}$	Φ_{trans}[f]	em, Φ_{trans}[g]	av, Φ_{trans}[h]
(BDPY)$_1$-*p*-Fb(**8**)	toluene	2.9	24	0.83	0.96	0.30	0.61	0.91	0.98	0.95
	CH_3CN	1.8	26	0.94	0.90	0.27	0.64	0.91		
(BDPY)$_1$-*p*-Zn (**Zn-8**)	toluene	2.0	17	0.90	0.94	0.27	0.67	0.94	1.02	0.98
	CH_3CN	0.4	8.0	0.98	0.97	0.34	0.63	0.97		
(BDPY)$_1$-*p*-Fb (**9**)	toluene	2.9	26	0.84	0.95	0.38	0.52	0.90	0.93	0.92
(BDPY)$_2$-*m*-Fb (**10**)	toluene	2.0	24	0.88	0.96	0.30	0.63	0.93	0.96	0.95
(BDPY)$_8$-*m*-Fb (**11**)	toluene	1.7	15	0.90	0.97	0.50	0.44	0.94	0.80	0.87
(BDPY)$_8$-*m*-Zn (**Zn-11**)	toluene	1.7	15	0.90	0.97	0.41	0.53	0.94	0.90	0.92

[a] Based on the data given in Table 3. [b] Using eq 1a. [c] Using eq 1b. [d] Using eq 2a. [e] Using eq 2b. [f] Using eq 3. [g] Average value from three different measurements using static emission spectroscopy: (1) emission from the Fb porphyrin for excitation at 516 vs 420 nm, (2) amplitudes of the fluorescence−excitation vs absorption intensities in the 516-nm BDPY band for spectra normalized in the Soret region, and (3) reduction in quantum yield of BDPY emission in the arrays relative to the BDPY-TMS reference compound. For a given complex, the highest and lowest values from the three measurements differed by no more than a yield of 0.13. [h] Average of the values from the transient absorption and static emission measurements in the previous two columns.

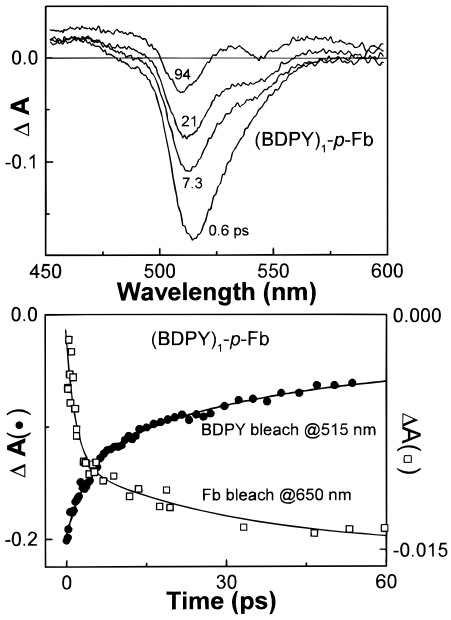

Figure 3. Representative room-temperature transient absorption and kinetic data for (BDPY)$_1$-*p*-Fb in toluene. In the lower panel, the closed circles are for decay of the bleaching in the BDPY band at 515 nm, and the open squares are for growth of the bleaching in the 650-nm $Q_x(0,0)$ absorption band of the Fb porphyrin; the solid lines are fits to a dual-exponential function. The resulting time constants (and relative amplitudes) are 2.4 ± 0.4 ps (36%) and 23 ± 2 ps (64%) at 515 nm, and 1.8 ±0.7 ps (45%) and 30 ± 6 ps (55%) at 650 nm.

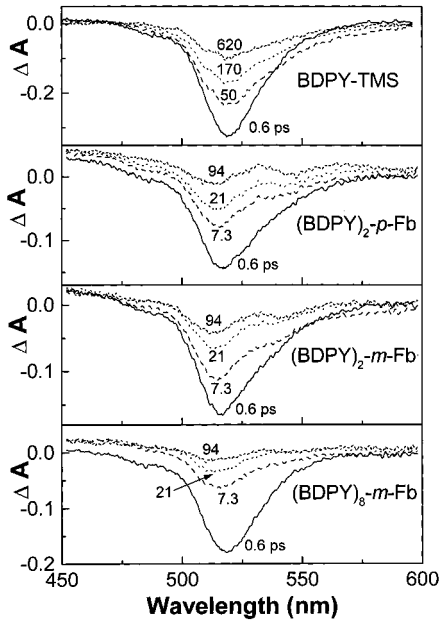

Figure 4. Representative transient absorption spectra for BDPY-TMS (top panel) and three Fb porphyrin-containing arrays with multiple BDPY pigments (lower three panels).

bleaching in the latter band and in the $Q_x(0,0)$ band near 650 nm is quite pronounced in long-time (but not early-time) spectra that extend to longer wavelengths and that were acquired on more concentrated samples using 480-nm excitation (spectra not shown).

The photoexcited BDPY constituent of (BDPY)$_1$-*p*-Fb exhibits a two-component decay, as reflected in the time evolution of the BDPY bleaching at 515 nm (solid circles in Figure 3, bottom panel). A fit of this decay with a dual-exponential function returned time constants of 2.4 ± 0.4 and 23 ± 2 ps with 36/64 relative amplitudes (Table 3). These kinetic components are found throughout the BDPY band. Furthermore, the growth of the Fb porphyrin bleachings exhibits the same dual-exponential behavior. This fact is most strongly seen from the measurements in the Fb porphyrin $Q_x(0,0)$ bleaching at 650 nm, which is well separated from the BDPY feature. These data are also shown in Figure 3 (open squares) along with a dual-exponential fit with time constants of 1.8 ± 0.7 and 30 ± 6 ps of roughly equal amplitude. These values for the Fb porphyrin bleachings are in good agreement with those found for decay of the BDPY bleaching considering the 10-fold smaller amplitude of the absorbance change obtained in the 650-nm porphyrin band and consequent large error limits.

The arrays containing multiple BDPY pigments per porphyrin give overall time-resolved absorption data similar to one another and to those of the mono-BDPY-containing arrays. Representative transient spectra for (BDPY)$_2$-*p*-Fb, (BDPY)$_2$-*m*-Fb, and (BDPY)$_8$-*m*-Fb in toluene, obtained using 513-nm excitation of the BDPY pigments, are shown in Figure 4. The corresponding kinetic traces for decay of the BDPY bleaching at 515 nm are given in Figure 5. Again, dual-exponential decays are observed. The time constants and amplitudes are generally comparable to those found for (BDPY)$_1$-*p*-Fb. However, some differences are indicated by the kinetic data: (1) The fast component of the decay of (BDPY)$_2$-*m*-Fb has a slightly smaller amplitude compared to that of (BDPY)$_2$-*p*-Fb. (2) The fast component of the decay of (BDPY)$_8$-*m*-Fb has a larger amplitude relative to those of the complexes having fewer BDPY pigments per porphyrin.

(b) Solvent Dependence Studies. The effects of different media on the photodynamics of various arrays were examined

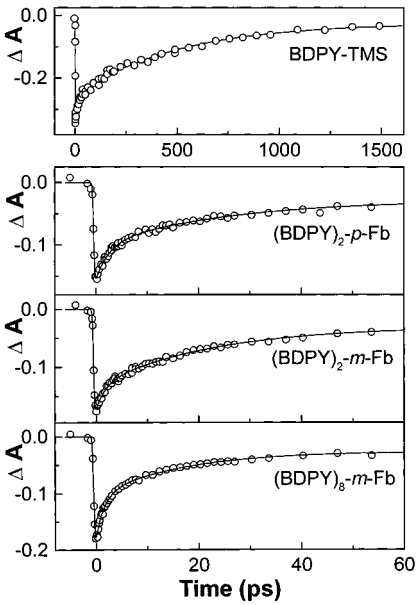

Figure 5. Kinetic data for BDPY-TMS (top panel) and three Fb porphyrin-containing arrays with multiple BDPY pigments (lower three panels). The data are for decay of the BDPY bleaching at 515 nm. The solid lines are fits to a dual-exponential function. The resulting lifetimes are given in Table 3.

using acetonitrile, dimethyl sulfoxide, and mineral oil. For $(BDPY)_1$-*p*-Fb, dual-exponential decays of the BDPY bleaching (513-nm excitation) were observed in each solvent, with time constants and amplitudes not appreciably different from those found in toluene (Table 3). A small solvent effect was observed for the excited Fb component of $(BDPY)_1$-*p*-Fb. The lifetime of the excited Fb component, which is formed via energy transfer from the excited BDPY moiety, is slightly faster in acetonitrile (8.5 ns) than in toluene (10.2 ns). The latter value and the lifetimes of the other arrays containing a Fb porphyrin (9.9−12.1 ns) are slightly shorter than the values of the Fb porphyrin reference monomers FbTPP and FbTMP (∼13 ns) in toluene (Table 3). These observations suggest that the excited Fb porphyrin in the arrays decays, in low yield, by an additional channel not available in the isolated porphyrin reference compounds. The shorter lifetime for the excited Fb porphyrin in $(BDPY)_1$-*p*-Fb in polar versus nonpolar solvents is consistent with the idea that this decay channel involves charge transfer between the excited Fb porphyrin and the BDPY pigment (vide infra). Boron-dipyrrin dyes have been shown to undergo photoinduced electron-transfer reactions.[36]

The effects of solvents on the photodynamics of the Zn chelate $(BDPY)_1$-*p*-Zn also were investigated (Table 3). The effects generally are quite similar to those with $(BDPY)_1$-*p*-Fb. The most notable difference is that both components of the decay of the photoexcited BDPY constituent of $(BDPY)_1$-*p*-Zn become significantly faster when the solvent is switched from toluene (1.8 and 16 ps) to acetonitrile (0.4 and 7.7 ps). This change in solvent also results in a dramatic shortening in the lifetime of the excited Zn porphyrin component of the array (from 2 ns in toluene to 34 ps in acetonitrile). The excited Zn porphyrin is formed via energy transfer from the photoexcited BDPY pigment. As in the case of the arrays containing a Fb porphyrin, these results are most readily explained in terms of charge transfer involving either the excited BDPY and ground-state porphyrin component or the excited porphyrin and the ground-state BDPY moiety. The more pronounced involvement of excited-state charge transfer in $(BDPY)_1$-*p*-Zn versus $(BDPY)_1$-*p*-Fb suggests oxidation (rather than reduction) of the porphyrin component, based on the fact that the Zn porphyrin in $(BDPY)_1$-*p*-Zn is easier to oxidize (but harder to reduce) than the Fb porphyrin in $(BDPY)_1$-*p*-Fb (Table 1). This trend parallels the differences in redox properties of isolated porphyrins.[33]

(c) Reference Compounds. The excited-state properties of several boron-dipyrrin reference compounds were examined for comparison with the arrays. The excited-state lifetime was assayed via decay of the bleaching in the blue-green ground-state absorption band in the same manner as described above for the arrays. Representative data for BDPY-TMS are shown in the top panels of Figures 4 and 5. The bleaching decay exhibits two phases, with time constants of 15 and 520 ps in toluene, with the latter comprising about 75% of the overall amplitude (Table 3). The decay components in 3-methylpentane are similar to those found in toluene. In the more polar solvent acetonitrile, the lifetime of the longer-lived component is reduced about 2-fold to 230 ps, and the fluorescence yield is concomitantly reduced.

While BDPY-TMS is the key reference compound against which the photodynamics of the BDPY-porphyrins are compared, several other boron-dipyrrin dyes were examined in order to gain a better understanding of the fundamental photophysics of this class of compounds. (1) The dye BDPY′, which lacks the ethyne group as well as the methyl groups at the 3- and 5-positions, exhibits two kinetic phases in toluene at room temperature that are similar to those found for BDPY-TMS. (2) When the ethynyl-TMS moiety of BDPY-TMS is replaced by the iodo group in BDPY-I, the lifetime of the long-lived component in toluene lengthens to 1.9 ns, and the fluorescence yield increases as well. (3) The pyrrole-substituted boron-dipyrrin complex, BODIPY, lacks the aryl group at the 5-position that is present in the arrays and in all the other reference compounds studied here. BODIPY exhibits a fast component ($\tau \sim 11$ ps) of amplitude 22% and a slow component (amplitude 78%) that does not decay over the 3.5-ns span of the transient absorption measurements. Time-resolved fluorescence spectroscopy showed this longer-lived component to have a time constant of 5.0 ns in toluene. This value is in good agreement with the fluorescence lifetime of 5.8 ns determined previously in ethanol.[19]

(6) Molecular Orbital Calculations. We used semiempirical molecular orbital theory[37,38] to probe the photophysical properties of the ground and excited states of *N*,*N*′-difluoroboryl-5-phenyldipyrrin (BDPY′) (Chart 2). The MNDO-AM1 method[37] was used to calculate the optimized geometries, and the MNDO-PSDCI method[38] was used to calculate the spectroscopic properties. Singly and doubly excited states from the π system were included in the excited-state calculations. The results are presented in Figure 6 [molecular conformation diagrams of the ground state (S_0) and the lowest excited singlet state (S_1)], Figure 7 (S_0 and S_1 potential energy contours), Figure 8 (S_0 and S_1 potential energy surfaces), and Figure 9 (molecular orbital diagrams). The characteristics of the ground- and excited-state surfaces are described below.

The ground state (S_0) is predicted to have only one stable conformer. In this conformer, the phenyl group is rotated 52° with respect to the rigorously planar dipyrrin framework (Figure 6A). Two equal energy minima, labeled **G** and **G**′, are indicated

(36) Wasielewski, M. R.; Debreczeny, M. P.; Svec, W. A. *Science* **1996**, *274*, 584−587.

(37) Dewar, M. J. S.; Zoebisch, E. G.; Healy, E. F.; Stewart, J. J. P. *J. Am. Chem. Soc.* **1985**, *107*, 3902−3909.

(38) Martin, C. H.; Birge, R. R. *J. Phys. Chem. A* **1998**, *102*, 852−860.

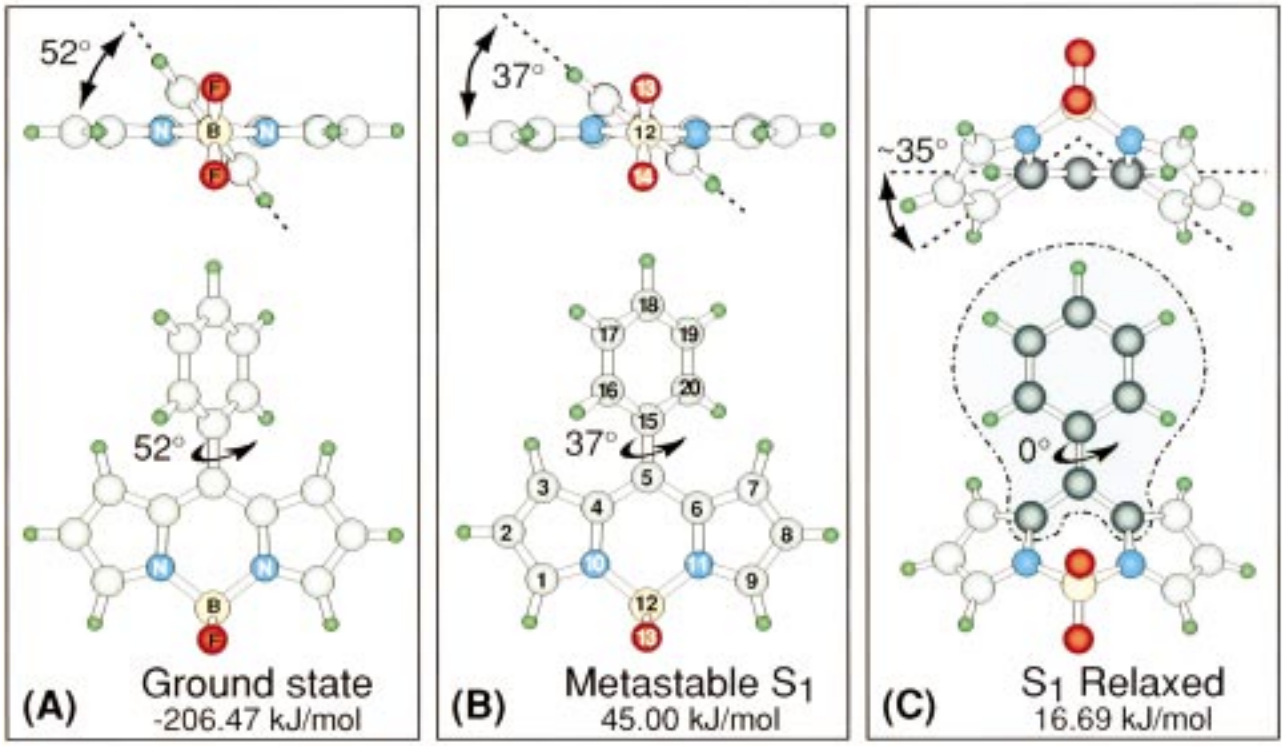

Figure 6. Equilibrium and metastable geometries in the ground (A) and lowest-excited singlet states (B, C). The atom numbering is shown in panel B, and the region of planarity in the lowest-energy conformation in S_1 (C) is outlined in light blue.

on the ground-state (S_0) contour map shown in Figure 7 because symmetry dictates that the conformers with phenyl torsional angles of 52° and 180° − 52° = 128° are isoenergetic.

The calculated surface of the lowest energy excited state (S_1) is significantly different from that of the ground state (S_0). In particular, the S_1 surface has multiple minima, some of which do not arise simply as a consequence of symmetry. One pair of minima on the S_1 surface corresponds to a metastable conformer (**M**) with a geometry very similar to the ground-state equilibrium geometry but with the phenyl ring rotated 37° (or 180° − 37° = 143°) with respect to a rigorously planar dipyrrin framework (Figure 6B, **M** and **M′** in Figure 7). The second set of minima on the S_1 surface has a lower energy and corresponds to a fully relaxed conformer (**R**) in which the phenyl ring is rotated into the plane defined by atoms 4, 5, and 6 and the dipyrrin frame is significantly distorted ($\omega \sim 35°$) out of that plane (Figure 6C). Symmetry considerations associated with the phenyl torsion in conjunction with the out-of-plane deformation of the dipyrrin skeleton (deformations with $\pm\omega$ are equivalent) dictate the existence of four isoenergetic conformers, labeled $\mathbf{R_1}$, $\mathbf{R_2}$, $\mathbf{R_1'}$, $\mathbf{R_2'}$, in Figure 7.

In the **R** conformer, the planarity of the 5-phenyl ring and the 5-carbon and the two adjacent α-pyrrole carbons causes considerable electron density to shift from the boron-dipyrrin chromophore onto the phenyl ring (Figure 9). Indeed, the observation that this highly distorted geometry is the lowest energy conformation of the excited state is due to resonance stabilization of the lowest unoccupied molecular orbital (LUMO). The MNDO-PSDCI configurational description of the lowest excited singlet state (S_1) indicates that this state is characterized as primarily a HOMO → LUMO configuration (~90%) mixed with a doubly excited (HOMO-1, HOMO → LUMO, LUMO) configuration (~6%). The energy of the excited state is influenced in large part by the energy of the LUMO [which is the highest energy singly occupied MO (HESOMO) in the variational S_1 state]. This orbital is distributed throughout the dipyrrin unit, with increasing stabilization as density is shifted onto the phenyl ring as the ring is rotated into the plane defined by atoms 4, 5, and 6 (see Figures 6C and 9). Due to the symmetry of this orbital, the principal bonding contribution is between atoms 5 and 15, which also drives the phenyl ring to seek a planar geometry. The occupation of the HESOMO orbital also increases antibonding between the extended phenyl conjugated system (atoms 4, 5, 6, and 15−20) and the remainder of the boron-dipyrrin unit. The combination of the above bonding and antibonding effects not only drives the phenyl ring into the plane but also allows the boron-dipyrrin system to seek a bent geometry in the **R** excited-state conformer.

Discussion

An ongoing theme of our studies of multiporphyrin arrays is the design and construction of architectures that are capable of capturing large amounts of impinging light and subsequently transferring the stored energy to a desired location. The control of these photophysical properties is requisite for the preparation of prototypical molecular photonic devices based on multiporphyrin architectures. For efficient light harvesting, the spectral coverage should be broad and/or tunable, which requires the incorporation of accessory pigments with absorption characteristics that complement those of the porphyrin components. For photonics applications, it could also be advantageous to place a number of accessory pigments near one specific porphyrin in a multiporphyrin array in order to enable selective input of photonic energy at that site. Our previous designs of multiporphyrin arrays used the *p*-aryl positions of tetraarylporphyrins as the site of interpigment connection,[2−5,8,10,11,14,24,31,39] thereby limiting each porphyrin to a maximum of four adjacent

(39) Fenyo, D.; Chait, B. T.; Johnson, T. E.; Lindsey, J. S. *J. Porphyrins Phthalocyanines* **1997**, *1*, 93−99.

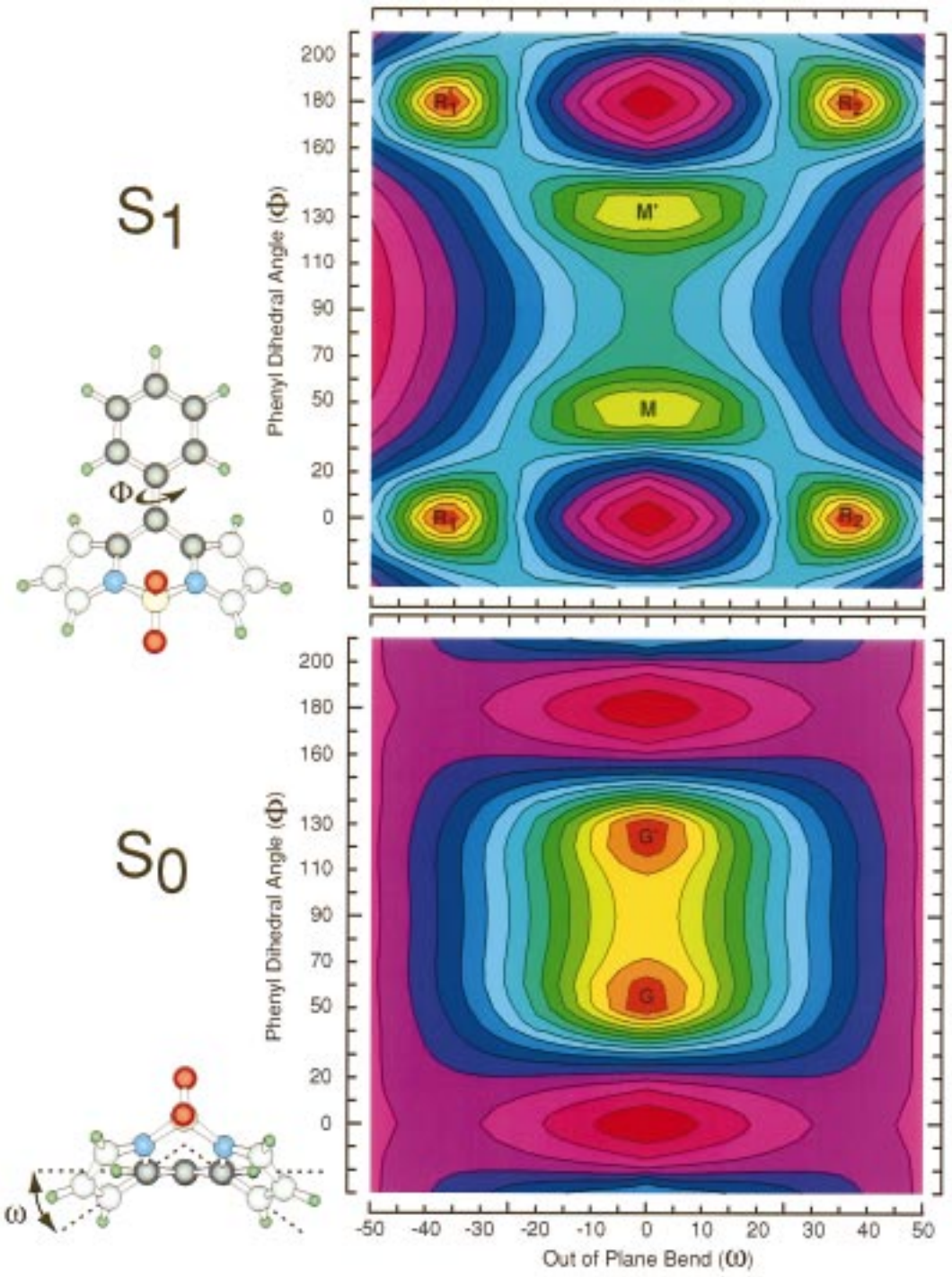

Figure 7. Adiabatic potential energy contours as a function of the phenyl group dihedral angle (Φ) and the out-of-plane deformation of the BDPY unit (ω). The contour regions are partitioned logarithmically, with energy increasing from lowest (orange) through yellow, green, blue, cyan, magenta, and red (highest). The minima marked **G** [in S_0 (lower) contour], **M** [in S_1 (upper) contour], and **R** [in the S_1 (upper) contour] correspond to the conformations shown in panels A, B, and C in Figure 6, respectively. The conformers labeled with primes are symmetric equivalents of the unprimed conformers. The $\mathbf{R}_1$ and $\mathbf{R}_1'$ conformers are symmetric equivalents of the $\mathbf{R}_2$ and $\mathbf{R}_2'$ conformers.

pigments. In the present study, we have developed strategies for connecting additional pigments via the *meta*-positions of the aryl rings. This approach has not been extensively exploited in the past[13,16,17,40−42] but enjoys the advantage that twice the number of interpigment connections can be established. The arrays reported herein containing one, two, or eight boron-dipyrrin pigments situated around a single free base or Zn porphyrin represent a new class of highly efficient light-harvesting assemblies that can serve as input elements in photonics applications.

Two key findings concerning the photophysical properties of the new class of BDPY-porphyrin arrays are as follows. (1) The strong blue-green absorption of the boron-dipyrrin accessory pigment complements the spectral characteristics of the Fb or Zn porphyrin. In the octa-BDPY complexes, the absorption intensity of the BDPY band rivals that of the porphyrin Soret band. (2) The energy-transfer process from the photoexcited BDPY units to the central porphyrin is highly efficient in all of the arrays (although the efficiency declines slightly upon incorporating eight BDPY units around the porphyrin). These

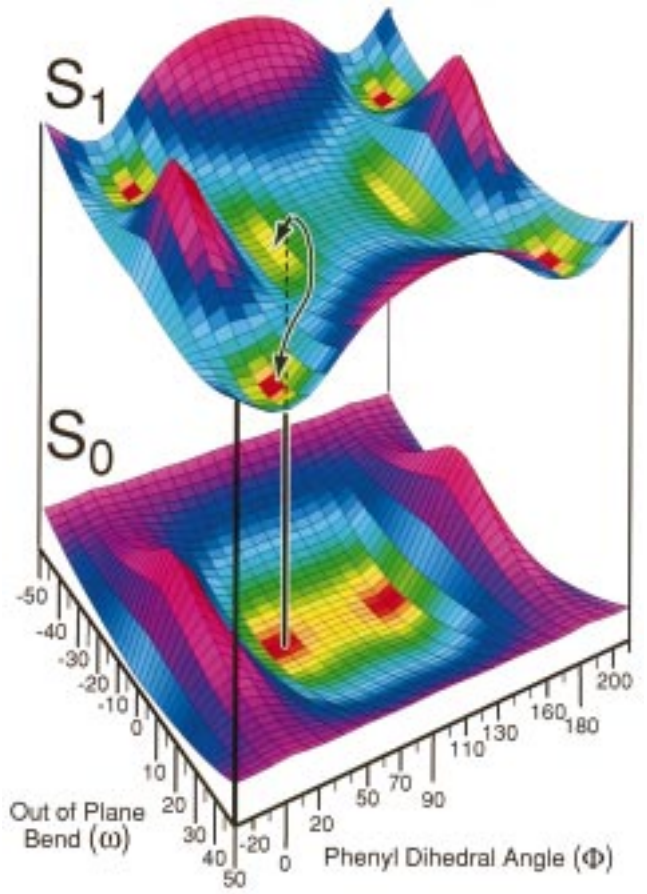

Figure 8. Adiabatic potential-energy surfaces as a function of the phenyl group dihedral angle (Φ) and the out-of-plane deformation of the BDPY unit (ω). The colors follow the same convention as in Figure 7. The vertical black line with the white outline shows the excitation process from the ground state into the Franck−Condon form of the excited state. The excitation process from the equivalent symmetry-related ground state conformer into its respective Franck−Condon excited state is not indicated. The short arrow on the S_1 surface shows decay into the metastable (**M**, Figure 6B) excited state. The long curved arrow shows decay into the relaxed (**R**, Figure 6C) excited state. Note that the **R** excited state is formed from the initial vibrationally/conformationally unrelaxed Franck−Condon form via ultrafast vibrational dynamics and relaxation and not from the vibrationally relaxed **M** state (see text and Figure 10).

two characteristics in and of themselves indicate that the BDPY-porphyrin arrays possess certain key properties required of suitable input elements for photonics applications. Nevertheless, the excited-state dynamics of the BDPY pigments (both isolated and in the arrays) are more complex than originally anticipated. These complexities and the properties of the BDPY pigments that influence the efficiency and mechanism(s) of energy transfer in the BDPY-porphyrin arrays are discussed in more detail below.

Structural, Electronic, and Photophysical Properties of the Boron-Dipyrrin Pigments. Free base dipyrrins such as bilins (e.g., bilirubin) exhibit very little fluorescence in fluid medium. However, high fluorescence yields are observed from these compounds in frozen solutions.[43] The enhanced fluorescence in the latter medium is attributed to the rigidification of the dipyrrin superstructure. Consistent with this notion, near-unity fluorescence is observed for bilin chromophores associated with the proteins in the phycobilisome antenna complexes of cyanobacteria.[44] In the boron-dipyrrin pigments, complexation of the dipyrrins with the boron-difluoride unit effectively locks the superstructure and affords a fluorescent chromophore. In particular, the 5-unsubstituted boron-dipyrrins (e.g., BODIPY) exhibit high fluorescence yields ($\Phi_f \sim 0.3-0.8$) and are widely used as biochemical probes. For this reason, we were surprised to find that the 5-aryl-substituted boron-dipyrrins used in the present study (e.g., BDPY-TMS) exhibit considerably smaller emission yields, in particular $\Phi_f \sim 0.05$.[22]

The disparity in the fluorescence yields in the BDPY versus BODIPY pigments points to the fact that the structural and electronic properties of this entire class of dyes are more complex than previously recognized. This view is amplified by a number of other observations: (1) The fluorescence quantum yield of the 5-unsubstituted boron-dipyrrin dyes varies considerably ($\Phi_f \sim 0.3-0.8$), depending on the type and number of the substituents at the α- and β-pyrrole carbons.[19,45] (2) Both 5-substituted and 5-unsubstituted boron-dipyrrin dyes exhibit multiple excited-state decay pathways. In the BDPY-porphyrin arrays, the relative magnitudes of the two components are roughly the same as in the 5-substituted boron-dipyrrin reference compounds (30/70), although the decay rates are shorter (∼2 and ∼15 ps versus ∼15 and ∼500 ps in BDPY-TMS) due to energy transfer. (3) The simple replacement of the ethynyl-TMS moiety of BDPY-TMS with the electron-withdrawing iodo substituent in BDPY-I causes an approximately 4-fold increase in the excited-state lifetime of the dominant component from ∼0.5 to ∼2 ns and a similar increase in fluorescence yield. (4) The blue-green absorption band of all the 5-substituted complexes including BDPY′ (which lacks α-methyl groups; Chart 2) is about 50% broader than the band in BODIPY (which in turn lacks the 5-aryl ring) (fwhm ∼ 25 versus 15 nm), and the shift between the respective absorption and emission maxima is about 4.5-times larger (∼700 versus ∼150 cm^{-1}). (5) The redox waves of the BDPY pigments are quite broad compared to those of other compounds (e.g., the porphyrin constituents). Collectively, the above-noted observations not only confirm the complexity of the structural, electronic, and photodynamic properties of the boron-dipyrrin chromophore, but also reveal that the introduction of a 5-aryl group strongly modulates these properties. In particular, this structural feature shortens the

(40) (a) Anderson, H. L.; Sanders, J. K. M. *J. Chem. Soc., Chem. Commun.* **1989**, 1714−1715. (b) Anderson, H. L.; Sanders, J. K. M. *Angew. Chem., Int. Ed. Engl.* **1990**, *29*, 1400−1403. (c) Anderson, S.; Anderson, H. L.; Sanders, J. K. M. *Angew. Chem., Int. Ed. Engl.* **1992**, *31*, 907−910. (d) Vidal-Ferran, A.; Müller, C. M.; Sanders, J. K. M. *J. Chem. Soc., Chem. Commun.* **1994**, 2657−2658. (e) Anderson, S.; Anderson, H. L.; Bahall, A.; McPartlin, M.; Sanders, J. K. M. *Angew. Chem., Int. Ed. Engl.* **1995**, *34*, 1096−1099. (f) Anderson, H. L.; Sanders, J. K. M. *J. Chem. Soc., Perkin Trans. 1* **1995**, 2223−2229. (g) Anderson, H. L.; Anderson, S.; Sanders, J. K. M. *J. Chem. Soc., Perkin Trans. 1* **1995**, 2231−2245. (h) Marvaud, V.; Vidal-Ferran, A.; Webb, S. J.; Sanders, J. K. M. *J. Chem. Soc., Dalton Trans.* **1997**, 985−990. (i) Vidal-Ferran, A.; Clyde-Watson, Z.; Bampos, N.; Sanders, J. K. M. *J. Org. Chem.* **1997**, *62*, 240−241.

(41) (a) Osuka, A.; Maruyama, K.; Yamazaki, I.; Tamai, N. *Chem. Phys. Lett.* **1990**, *165*, 392−396. (b) Maruyama, K.; Kawabata, S. *Bull. Chem. Soc. Jpn.* **1990**, *63*, 170−175. (c) Osuka, A.; Kobayashi, F.; Maruyama, K. *Bull. Chem. Soc. Jpn.* **1991**, *64*, 1213−1225. (d) Osuka, A.; Liu, B.; Maruyama, K. *J. Org. Chem.* **1993**, *58*, 3582−3585. (e) Officer, D. L.; Burrell, A. K.; Reid, D. C. W. *J. Chem. Soc., Chem. Commun.* **1996**, 1657−1658. (f) Amabilino, D. B.; Sauvage, J.-P. *J. Chem. Soc., Chem. Commun.* **1996**, 2441−2442.

(42) Lindsey, J. S. In *Metalloporphyrin-Catalyzed Oxidations*; Montanari, F., Casella, L. Eds.; Kluwer Academic Publishers: The Netherlands, 1994; pp 49−86.

(43) Greene, B. I.; Lamola, A. A.; Shank, C. V. *Proc. Natl. Acad. Sci. U.S.A.* **1981**, *78*, 2008−2012.

(44) Glazer, A. N. *Biochim. Biophys. Acta* **1984**, *768*, 29−51.

(45) (a) Vos de Wael, E.; Pardoen, J. A.; von Koeveringe, J. A.; Lutenburg, J. *Recl. Trav. Chim. Pays-Bas* **1977**, *96*, 306−309. (b) Holzwarth, A. R.; Lehner, H.; Braslavsky, S. E.; Shaffner, K. *Liebigs. Ann. Chem.* **1978**, 2002−2017.

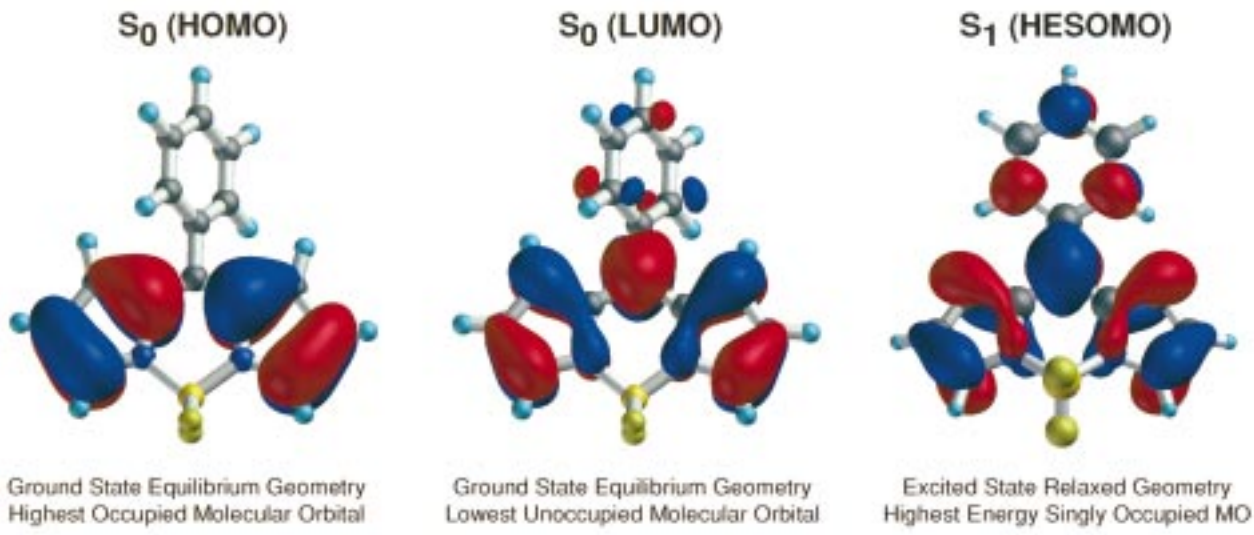

Figure 9. Molecular orbitals in the S_0 (left and middle) and S_1 (right) states of BDPY. Sign reversal of the wave function is reflected by red and blue regions.

lifetime of the dominant excited-state decay pathway and enhances the contribution of a fast excited-state deactivation route (Table 4), which in turn modulates the energy-transfer channels in the BDPY-porphyrin arrays.

The molecular orbital calculations on the simple boron-dipyrrin complex substituted with only a 5-phenyl ring (i.e., BDPY′) give a clear physical basis for understanding the photophysical properties of the complexes. A model consistent with all the static and time-resolved optical data can be discussed with the aid of Figure 10, which shows a schematic pseudo-one-dimensional slice through the multidimensional potential energy surfaces shown in Figure 8. Photoexcitation of the ground electronic state in its equilibrium geometry (**G** or **G′**) near the 515-nm absorption maximum initially prepares the lowest excited singlet state with the same geometry as the ground state, namely a planar boron-dipyrrin unit with a phenyl torsional orientation of 52° (or 180° − 52° = 128°) (Figure 6A, vertical black and white line in Figure 7, vertical black arrows in Figure 10). This initial Franck−Condon form of the S_1 electronic excited state has a geometry closer to that of the metastable (**M** or **M′**) conformer than that of the fully relaxed (**R** or **R′**) conformer because the **M** conformer is characterized by a planar boron-dipyrrin framework with a phenyl torsional angle that is only modestly smaller ($\Phi \sim 37°$; Figure 6B). In contrast, the **R** conformer differs by a substantial additional reduction in this torsional angle ($\Phi \sim 0°$) along with a significant distortion of the boron-dipyrrin framework from planarity ($\omega \sim 35°$) (Figure 6C). The initially photoprepared Franck−Condon form of the excited state will be vibrationally/conformationally unrelaxed with respect to both the phenyl-dipyrrin torsional motion and the out-of-plane deformation of the boron-dipyrrin unit. This Franck−Condon form will contain contributions from a number of vibronic states on the S_1 surface. These vibronic states include those which exhibit probability amplitude in the region of both the **M** and **R** conformers. Both conformers are excited due to the characteristics of the excitation pulse relative to the ∼800-cm^{-1} barrier between the **M** and **R** conformers: (1) The observation of a 700-cm^{-1} Stokes shift between the absorption and emission maxima dictates that the 515-nm excitation pulse will access vibronic components on the S_1 surface that are close to, if not above, the **M**−**R** barrier. (2) The ∼120-fs pulse has a spectral dispersion (∼250 cm^{-1}) that is a significant fraction of the **M**−**R** barrier. Two of the many vibronic eigenstates on the S_1 surface that are initially accessed are shown in Figure 10. The lower energy eigenstate has significant probability amplitude in the Franck−Condon

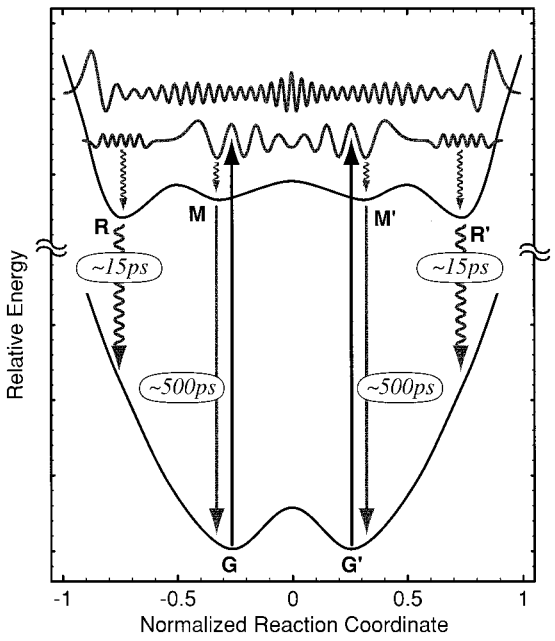

Figure 10. Pseudo one-dimensional slice through the ground-state (S_0) and excited-state (S_1) potential energy surfaces shown in Figure 8. This figure also schematically summarizes the model for the excited-state dynamics that gives a consistent explanation of all the static and time-resolved optical data. The black vertical arrows indicate excitation of the **G** (or **G′**) conformers to the respective Franck−Condon forms of the excited state. Two of the many vibrational eigenstates that will contribute to the initially prepared excited-state are indicated. The lower energy eigenstate has significant probability amplitude in the Franck−Condon region, while the upper state has substantially more probability amplitude outside this region. Note that both of these vibrational eigenstates have significant probability amplitude in the regions of both the **M** (or **M′**) and **R** (or **R′**) excited-state conformers. Vibrational relaxation to **M** and **R** in their respective potential energy minima is indicated by the short wavy arrows. Subsequently, the **M** (or **M′**) conformer decays by both emission and nonradiative decay with an overall lifetime of about 500 ps (gray vertical arrows), while the **R** (or **R′**) conformer decays primarily nonradiatively with a lifetime of about 15 ps (large wavy arrows).

region, whereas the higher energy eigenstate has larger probability amplitude farther from the Franck−Condon region. However, both eigenstates exhibit probability amplitude in regions of both the **M** and **R** conformers.

The time-domain equivalent of the picture described above is as follows. The initial Franck−Condon form of the excited state is characterized by a wave packet that undergoes very rapid (subpicosecond) evolution along one or both of the torsional or out-of-plane configurational coordinates. During this evolution, the wave packet will sample regions of configurational space corresponding to both the metastable (**M**) and fully relaxed (**R**) conformers. Vibrational relaxation occurring on the time scale of several picoseconds or less (indicated by the short wavy arrows in Figure 10) will generate the **M** and **R** conformers with the equilibrium geometries and energies dictated by the respective minima on the S_1 potential energy surface (Figures 6B, 6C, 8, and 10). The branching into the **M** versus **R** conformations will be dictated by a number of factors, including the energy and trajectory of the initial excited-state wave packet as well as the relative motions required for the formation of the respective configurations. The significantly lesser extent of motion required to reach the **M** versus **R** conformation would greatly favor the former. Additionally, the initial Franck−Condon form of the excited state, having predominantly **M** character, could traverse a modest barrier to access the **M′** region of the conformational surface, and vice versa (Figures 8 and 10). Such motion would again favor ultimate branching into the **M** versus **R** conformer. Once the **M** (or **M′**) and **R** (or **R′**) conformers are formed on the ultrafast time scale, there will be little conversion between them due to the intervening barriers. The two excited-state conformers will then decay essentially independently, with lifetimes dictated by the respective radiative and nonradiative rate constants. When the porphyrin is appended, energy transfer to this moiety will also contribute to the observed lifetime. It must be emphasized that all of the decay processes, including energy transfer to the appended porphyrin, are slow compared with the formation of the **M** and **R** conformers.

The differences in the physical and electronic structures of the two excited-state conformers and their relationships to the ground-state structure provide detailed insights into the experimental observations. (1) The presence of two excited-state conformers that are energetically accessible following photoexcitation provides a rationale for the presence of two excited-state decay components in both the isolated boron-dipyrrin pigments (e.g., BDPY-TMS) and the BDPY-porphyrin arrays. [The presence of multiple ground-state conformers may also contribute to the photophysics, but the contribution is expected to be much smaller than that arising from the excited-state conformers due to the relevant energy gaps.] (2) The finding that the two excited-state decay components have similar relative magnitudes (30% fast and 70% slow) in the isolated pigments and the arrays is consistent with a lack of perturbation of the structure, orientation, or vibrational characteristics of the BDPY unit upon attachment to the porphyrin (see Chart 2).[46] In particular, according to the model for the excited-state dynamics presented above, the branching ratio between the **M** and **R** conformers is dictated by factors that should not differ significantly in the presence of the appended porphyrin. (3) The similarity in the physical and electronic structures of the ground state and **M** excited state, compared with the disparities between the ground state and **R** excited state, argues that the **M** excited state is more strongly radiatively coupled to the ground state than is the **R** excited state. In other words, the significant redistribution of electron density between the ground state and the **R** excited state causes radiative transitions between the two states to be very weak due to poor electronic overlap. Hence, transitions between the ground state and the **M** excited state dominate the 515-nm absorption band and the associated 535-nm fluorescence band. (4) The small BDPY-aryl reorientation that occurs between the ground state and the **M** excited state (52° versus 37° at the equilibrium positions) could account in part (or entirely) for the increased breadth of the 515-nm absorption band of the 5-aryl-substituted boron-dipyrrin pigments relative to the 5-unsubstituted analogues (∼25 versus ∼15 nm), as well as for the larger shift between the absorption and emission maxima (∼700 versus ∼150 cm^{-1}). (5) The difference in the BDPY-aryl torsional angle in the **M** versus ground state would also increase the Franck−Condon overlap and nonradiative decay rate of the **M** conformer relative to the situation for the 5-unsubstituted boron-dipyrrin pigments. Hence, this excited-state distortion mechanism can account for the shorter lifetime of the predominant (**M**) form of the S_1 state of BDPY-TMS relative to that of BODIPY (500 ps versus 2 ns) and contribute to the corresponding difference in fluorescence yields (Table 3). (6) The significantly larger structural displacement that occurs between the ground state and the **R** excited state at their equilibrium geometries would increase the Franck−Condon overlap and the nonradiative decay rate of the **R** excited state relative to those of the **M** excited state. The vibrational overlap factor in the **R** excited state is further enhanced because of the reduced vertical energy gap between that state and the ground state. Hence, the fast (∼15 ps) component of the excited-state decay in the isolated BDPY pigments can be assigned to the **R** excited state and the slow (∼500 ps) component of the decay to the **M** excited state. These assignments are consistent with the view that the **M** excited state in the 5-aryl-substituted boron-dipyrrin pigments is a "light" state (decays in part by fluorescence) due to its modestly long lifetime, whereas the **R** excited

(46) The assessment that the attachment of the BDPY unit to porphyrin does not appreciably alter the structural and/or electronic properties of either is derived from the observation that the optical spectra and redox properties of the constituent units are generally quite similar to those of the isolated components. In addition, the excited-state lifetimes and fluorescence yields of the porphyrin components of the arrays are generally similar to those found for the reference compounds (except in situations such as in polar solvents, where photoinduced charge transfer in the array may be significant). Thus, the electronic coupling between the BDPY pigments and the porphyrin core is relatively weak. It should be noted, however, that the presence of such a large number of boron-dipyrrin pigments in $(BDPY)_8$-*m*-Fb and $(BDPY)_8$-*m*-Zn appears to slightly perturb the electronic/structural properties of the porphyrin constituent. In particular, the Soret band in both of these arrays is red-shifted by about 10 nm relative to the arrays containing one or two BDPY units and to the reference porphyrins. One possible explanation is that the presence of eight BDPY units causes a small structural distortion of the porphyrin core, such as a deviation of the porphyrin macrocycle from planarity. Nonplanar distortions can cause substantial (over 50 nm) red shifts in the Soret and Q-bands of porphyrin chromophores.[a,b] If large enough, these distortions can be accompanied by significantly reduced excited-state lifetimes and emission yields, with the extent of the electronic perturbations depending on the type and degree of the structural modification.[c,d] However, the excited-state lifetimes and emission yields in the octa-BDPY-containing arrays are again similar to those of the isolated porphyrins. These findings and considerations imply that the structural distortions or other factors that underlie the modest Soret shifts for the octa-BDPY-containing arrays are insufficient to significantly alter the excited-state dynamics of the porphyrin core. (a) Barkigia, K. M.; Renner, M. W.; Furenlid, L. R.; Medforth, C. J.; Smith, K. M.; Fajer, J. *J. Am. Chem. Soc.* **1993**, *115*, 3627−3635. (b) Jentzen, W.; Simpson, M. C.; Hobbs, J. D.; Song, X.; Ema, T.; Nelson, N. Y.; Medforth, C. J.; Smith, K. M.; Veyrat, M.; Mazzanti, M.; Ramasseul, R.; Marchon, J.-C.; Takeuchi, T.; Goddard, W. A., III; Shelnutt, J. A. *J. Am. Chem. Soc.* **1995**, *117*, 11085−11097. (c) Gentemann, S.; Medforth, C. J.; Forsythe, T. P.; Nurco, D. J.; Smith, K. M.; Fajer, J.; Holten, D. *J. Am. Chem. Soc.* **1994**, *116*, 7363−7368. (d) Gentemann, S. G.; Nelson, N. Y.; Jaquinod, L. A.; Nurco, D. J.; Leung, S. H.; Smith, K. M.; Fajer, J.; Holten, D. *J. Phys. Chem. B* **1997**, *101*, 1247−1254.

state is essentially a "dark" state due to its very short lifetime. (7) The shift in electron density onto the 5-aryl ring in the **R** excited state causes this state to have a significantly larger electronic overlap and energy-transfer rate to the appended porphyrin in the arrays relative to the **M** excited state [$\sim$(2 ps)$^{-1}$ versus $\sim$(20 ps)$^{-1}$]. Hence, the differences in structure and electron density distributions between the two excited-state conformers explain why the fast decay component in the isolated pigments (dominated by deactivation to the ground state) correlates with the fast decay component in the arrays (dominated by energy transfer to the porphyrin), and similarly for the slow decay components.

Finally, we note that, while the picture described above can account for all of the spectroscopic and photophysical properties of the BDPY and BDPY-porphyrin arrays, it is, no doubt, an oversimplification of the processes that occur on the multidimensional excited-state surface. It should also be noted that certain alternative pictures cannot account for all of the observations. For example, the barrier between the **M** and **R** states must be relatively modest (as predicted by the calculations), or else the **R** state could not be accessed by the initially prepared vibrationally/conformationally unrelaxed wave packet. Likewise, the reverse assignment of the long-lived (radiative) excited state as **R** and the short-lived (dark) excited state as **M** would be contrary to the standard view that highly distorted excited states (such as **R**) generally access more nonradiative decay channels than relatively undistorted states (such as **M**).

Energy-Transfer Properties of the BDPY-Porphyrin Arrays. Static fluorescence measurements indicate that energy transfer in the BDPY-porphyrin arrays is >90% for the complexes containing one or two accessory pigments and 80−90% in the octa-substituted arrays. Due to the high yields of energy transfer, a more precise evaluation of the yield is best assessed through time-resolved measurements. These measurements reveal the presence of a (minimally) dual-exponential decay of the photoexcited BDPY constituent of the array. A similar dual-exponential rise is found for the formation, via energy transfer, of the excited Fb porphyrin constituent. As noted above, we attribute the fast kinetic component with the lower energy **R** excited-state conformer of the BDPY pigment and the slow kinetic component with the higher energy **M** excited-state conformer. Thus, for each array, two energy-transfer rate constants (k_{trans}) and efficiencies (ϕ_{trans}) can be calculated, using the following formulas:[47]

$$k_{trans(R)} = (\tau_R)^{-1} - (\tau_R{}^o)^{-1} \quad (1a)$$

$$k_{trans(M)} = (\tau_M)^{-1} - (\tau_M{}^o)^{-1} \quad (1b)$$

$$\phi_{trans(R)} = k_{trans(R)}\,\tau_R \quad (2a)$$

$$\phi_{trans(M)} = k_{trans(M)}\tau_M \quad (2b)$$

$$\Phi_{trans} = \chi_R\phi_{trans(R)} + \chi_M\phi_{trans(M)} = \chi_R\,k_{trans(R)}\,\tau_R + \chi_M\,k_{trans(M)}\tau_M \quad (3)$$

Here, τ_R and τ_M are the time constants of the fast and slow components of the BDPY excited-state decays in the BDPY-porphyrin array, associated with the **R** and **M** excited-state conformers, respectively. χ_R and χ_M are the respective amplitudes, and $\tau_R{}^o$ and $\tau_M{}^o$ are the lifetimes of the corresponding components in the reference compound BDPY-TMS. The overall energy-transfer yield (Φ_{trans}) is the sum of the yields from the two components ($\phi_{trans(R)}$, $\phi_{trans(M)}$) weighted by their amplitudes. This analysis yields $k_{trans(R)} \sim$ (2 ps)$^{-1}$ for the minor ($\chi_R = 0.30$) component and $k_{trans(M)} \sim$ (20 ps)$^{-1}$ for the dominant ($\chi_M = 0.70$) component in the BDPY-porphyrin arrays. Thus, even though energy transfer from the short-lived component in each array competes with an inherent deactivation time of only $\sim$15 ps, the process is highly efficient ($\phi_{trans(R)} = 83-90\%$), although not as efficient as that for the longer-lived predominant component ($\phi_{trans(M)} = 90-97\%$). The calculated values of the energy-transfer efficiencies and rate constants derived from the time-resolved measurements are given in Table 4. The last column in this table gives an average value of the energy-transfer efficiency in each array, derived from the independent static fluorescence and time-resolved measurements. We believe that these average values best represent the overall Φ_{trans} values in the respective arrays, given the individual assumptions and errors associated with the various measurements.

Our prior studies of diarylethyne-linked multiporphyrin arrays showed that the energy-transfer process is dominated by a TB mechanism mediated by the linker. In addition to a number of experimental observables, one factor underlying this conclusion is that the calculated Förster TS rate [$\sim$(1 ns)$^{-1}$] is significantly slower than the observed energy-transfer rate [<(100 ps)$^{-1}$] in the multiporphyrin arrays. In the case of the BDPY-porphyrin arrays, the rates of Förster transfer from the photoexcited BDPY pigments to the porphyrin core are estimated to be much faster, on the order of (100 ps)$^{-1}$ or greater (Appendix). The 10-fold faster Förster rate for BDPY-porphyrin energy transfer compared with porphyrin−porphyrin energy transfer arises from the combined effects of stronger resonance coupling (i.e., increased spectral overlap) and shorter interchromophore spacing. The closeness of the estimated Förster rates to the observed rate for the major component [$\sim$(20 ps)$^{-1}$], but perhaps less so for the minor component [$\sim$(2 ps)$^{-1}$], indicates that this mechanism probably plays a significant role in the photodynamics of the BDPY-porphyrin arrays.

Although TS Förster energy transfer most likely contributes to the overall energy transfer in the BDPY-porphyrin arrays, the experimental evidence strongly suggests that TB energy transfer is most likely the dominant contributor. This conclusion is derived from the following considerations: (1) The rates of energy transfer are essentially the same for arrays in which the connections of the BDPY unit are at the *meta*- versus *para*-position on the *meso*-aryl ring of the linker to the porphyrin core. If the Förster TS mechanism exclusively applied, observable differences in the energy-transfer rates and efficiencies for the different architectures would be expected (Appendix). Such differences are not observed (Tables 3 and 4). (2) Under the model presented above, the TS mechanism could not account for the $\sim$(2 ps)$^{-1}$ rate of energy transfer observed for the "fast" component of the array. (3) The TB mechanism must necessarily operate if energy transfer occurs, at least in part, via a state that is only very weakly radiatively coupled to the ground state, as appears to be the case for the short-lived excited-state component of the BDPY unit. (4) A contribution of the TB mechanism applies if the two kinetic components of energy

(47) Although there may be more than two kinetic components, only two are resolved, and hence, others cannot be uniquely determined. Furthermore, the treatment assumes there is no energy transfer among the BDPY units within a given array, which would mask a rate of transfer faster than the measured lifetime (see: Pearlstein, R. M. *Photochem. Photobiol.* **1982**, *35*, 835−844). We also neglect potential excited-state annihilation processes that could occur in the multi-BDPY-containing complexes if more than one BDPY were photoexcited in the same array. However, the finding of such similar photophysical behavior for the various BDPY-porphyrin arrays rules out any significant contribution of such multiphoton effects.

transfer observed in the arrays indeed reflect structural/electronic components having different electron density distributions (and thereby different electronic coupling through the bridge). As noted above, our model suggests that the 10-fold difference in the rate of energy transfer between the two excited-state components derives from structural-induced differences in the electron density on the 5-aryl ring that is integral to the linker in the arrays. Hence, the studies presented herein suggest that the TB energy-transfer mechanism makes a substantial if not dominant contribution to energy transfer between the photoexcited BDPY units and the porphyrin constituents in the arrays. This conclusion parallels that drawn previously from our studies of energy transfer between porphyrins also joined by diarylethyne linkers.

Conclusions

Energy transfer from the photoexcited BDPY accessory pigments to the porphyrin in the BDPY-porphyrin arrays is a highly efficient process. Furthermore, the optical properties of the boron-dipyrrin accessory pigments are highly complementary to those of the porphyrin, enhancing the light-harvesting properties of the arrays and facilitating selective excitation of the accessory pigment for other applications. The arrays with equal numbers of BDPY units at *p*- or *m*-aryl positions exhibit similar photochemical properties. The theoretical predictions concerning the excited-state properties of the boron-dipyrrin pigments afford a consistent explanation for all the experimental observations on both the isolated chromophores and the BDPY-porphyrin arrays. These considerations also highlight the central role played by the 5-aryl ring in the overall photodynamics of the compounds. The factors discussed here also raise the possibility that a closer relationship exists between our BDPY-porphyrin light-harvesting arrays and the natural light-harvesting systems than originally envisaged. In particular, carotenoids and related accessory pigments, like all linear polyenes, have multiple excited states that differ substantially in their electronic nature, electron density distributions, radiative and nonradiative deactivation properties, and rates of energy transfer to the (bacterio)chlorophyll components of the antenna systems.[48] However, the boron-dipyrrin dyes are readily synthesized and can be introduced into multipigment arrays via a modular building block approach. Accordingly, the BDPY-porphyrin constructs are excellent candidates for inclusion in light-harvesting model systems and as input elements of prototypical molecular photonic devices.

Acknowledgment. This work was supported by a grant from the Division of Chemical Sciences, Office of Basic Energy Sciences, Office of Energy Research, U.S. Department of Energy (J.S.L.), and grants from the NSF (CHE-9707995 to D.F.B., D.H., and J.S.L.; and CHE-9504697, postdoctoral fellowship, to C.H.M.) and the NIH (GM 34685 to D.H. and GM-34548 to R.R.B.). D.K. was supported by the Creative Research Initiative Program of the Ministry of Science and Technology of Korea. Partial funding for the Mass Spectrometry Laboratory for Biotechnology at North Carolina State University was obtained from the North Carolina Biotechnology Center and the NSF.

Appendix: Förster Energy-Transfer Calculations

The Förster energy-transfer rate is given by

$$k_{trans} = (8.8 \times 10^{23})\kappa^2 \Phi_f J n^{-4} \tau^{-1} R^{-6} \qquad \text{(A1)}$$

Here, k^2 is the orientation factor, Φ_f is the fluorescence quantum yield of the donor in the absence of the acceptor, J is the spectral overlap term (in $cm^6\ mmol^{-1}$), n is the solvent refractive index (1.496 for toluene), τ is the donor fluorescence lifetime (in ns) in the absence of the acceptor, and R is the donor-acceptor center-to-center distance (in Å).[49]

We make several assumptions in the Förster energy-transfer calculation. First, we neglect corrections to the point−dipole approximation when the donor−acceptor distance is comparable to the size of the donor−acceptor π system. Second, we ignore the effects of bending of the diarylethyne linkage[31] on the value of κ^2. Third, we assume the conformationally averaged dynamic limit where each donor−acceptor (BDPY-porphyrin) pair samples all internal rotation angles about the cylindrically symmetric ethyne bond. In the case of the *para*-substituted BDPY porphyrins, the ethyne, porphyrin−aryl, and BDPY−aryl bonds are all coaxial. Accordingly, the dynamically averaged value of κ^2 can be calculated with certainty. In contrast, for the *meta*-substituted BDPY porphyrins, the porphyrin−*meso*-aryl bond is not coaxial with the ethyne and boron-dipyrrin−5-aryl bonds. Thus, averaging about both axes must be considered to determine the value of κ^2. However, in the absence of detailed knowledge of the potential surface for torsional motion about the porphyrin−*meso*-aryl bond, it is not possible to uniquely assess an effective value of κ^2. Thus, we estimate κ^2 on the basis of the values obtained for specific torsional angles (see below).

With the above assumptions, the value of κ^2 can be calculated using the equation $\kappa^2 = (\cos\theta_T - 3\cos\theta_D \cos\theta_A)^2$. Here, θ_T is the transfer angle between the transition dipole vectors of the donors and the acceptor, and θ_D and θ_A are the angles that the transition dipole vectors of the donors and the acceptor make with the separation vector, respectively.[50] The transition dipole of BDPY lies along its longitudinal axis.[19] The Zn porphyrin is a planar oscillator, whereas the Fb porphyrin is a linear oscillator, with the transition dipole moment located along the N−N diagonal axis in the plane of the porphyrin.[51] For *para*-substituted BDPY porphyrins **8**, **Zn-8**, and **9**, the κ^2 value ranges from 0 (BDPY and porphyrin transition dipole moments are perpendicular) to 0.5 (BDPY and porphyrin transition dipole moments are coplanar). Dynamic averaging gives a κ^2 value of 0.25. For *meta*-substituted BDPY porphyrins **10**, **11**, and **Zn-11** with the *meso*-aryl ring fixed perpendicular to the porphyrin, rotation of the BDPY unit about the ethyne causes the κ^2 value to range from 0.5 (BDPY dipole perpendicular to the plane of the *meso*-aryl ring) to 0.63 (BDPY parallel to the plane of the *meso*-aryl ring). However, rotation of the aryl ring of the porphyrin toward coplanarity with the porphyrin causes a concomitant decrease in the upright orientation of the BDPY unit. CPK models indicate that a range of conformational space can be explored, including nearly coplanar and perpendicular geometries of the porphyrin and BDPY unit upon combinations of rotation about the porphyrin−*meso*-aryl ring bond and slight bending of the diarylethyne linker. In general, these motions cause the κ^2 value to be attenuated. Consequently, we have chosen a κ^2 value of 0.5 for the calculations on the *meta*-substituted complexes. This value was chosen because it most

(48) (a) Hudson, D. S.; Andrews, J. R. *J. Chem. Phys.* **1978**, *68*, 4587−4594. (b) Bennett, J. A.; Birge, R. R. *J. Chem. Phys.* **1980**, *73*, 4234−4246. (c) Birge, R. R. *Acc. Chem. Res.* **1986**, *19*, 138−146. (d) Kohler, B. E. *J. Chem. Phys.* **1990**, *93*, 5838−5842. (e) DeCoster, B.; Christensen, R. L.; Gebhard, R.; Lutenburg, J.; Farhoosh, R.; Frank, H. A. *Biochim. Biophys. Acta* **1992**, *1102*, 107−114.

(49) Lamola, A. A. In *Energy Transfer and Organic Photochemistry*; Lamola, A. A., Turro, N. J. Eds.; Interscience: New York, 1969; p 17.

(50) Dale, R. E.; Eisinger, J. *Biopolymers* **1974**, *13*, 1573−1605.

(51) (a) Gurinovich, G. P.; Sevchenko, A. N.; Solov'ev, K. N. *Opt. Spectrosc.* **1961**, *10*, 396−401. (b) Gouterman, M.; Stryer, L. *J. Chem. Phys.* **1962**, *37*, 2260−2266.

Table 5. Förster Energy-Transfer Parameters and Rates

array	κ^2 [a]	J (cm^6 mmol^{-1})[b]	R (Å)[c]	$(k_{trans})^{-1}$ (ps)[b]
$(BDPY)_1$-*p*-Fb (**8**)	0.25	7.0×10^{-14}	18	99
$(BDPY)_1$-*p*-Zn (**Zn-8**)	0.25	1.3×10^{-13}	18	53
$(BDPY)_2$-*p*-Fb (**9**)	0.25	7.0×10^{-14}	18	99
$(BDPY)_2$-*m*-Fb (**10**)	0.5	7.0×10^{-14}	15	17
$(BDPY)_8$-*m*-Fb (**11**)	0.5	7.0×10^{-14}	15	17
$(BDPY)_8$-*m*-Zn (**Zn-11**)	0.5	1.3×10^{-13}	15	9

[a] Assuming the dynamic averaged limit for the *para*-substituted complexes and a rough average value for the *meta*-substituted complexes (see text). [b] Based on the emission properties of BDPY-TMS and the absorption properties of FbTPP or ZnTPP. [c] Based on CPK models.

likely overestimates the actual dynamically averaged value and, thus, the rate of TS energy transfer.

A program and accompanying spectral database were used to perform the Förster calculations.[52] Calculations of the energy-transfer rate (k_{trans}) using eq A1 were carried out only for the dominant, slower kinetic component for the BDPY-TMS reference complex. Thus, a value of $\tau = 520$ ps is employed for the lifetime of the photoexcited BDPY energy-transfer donor in the absence of the acceptor. Similarly, we use $\Phi_f = 0.058$ for the corresponding fluorescence yield under the assumption that the observed emission is associated with this component. Furthermore, we assume that the absorption and emission spectra (which yield the spectral overlap terms) arise predominantly from the BDPY component associated with the dominant slow kinetic component. The results of the calculations performed using the various assumptions are summarized in Table 5. It should be noted that, given the assumption and uncertainties associated with these calculations (particularly for the *meta*-substituted complexes), the derived values of k_{trans} are intended only as rough estimates. The purpose is to assess whether the Förster rate is sufficiently close to the observed energy-transfer rates that the TS mechanism plays an appreciable role in the photodynamics of these arrays.

(52) Du, H.; Fuh, R.-C. A.; Li, J.; Corkan, L. A.; Lindsey, J. S. *Photochem. Photobiol.* **1998**, *68*, 141−142.

Supporting Information Available: Experimental section, including synthetic procedures for 13 compounds, chart of compounds, and ^{1}H NMR spectra for **1**, **7**, **8**, **9**, **11** and **Zn-11** (21 pages, print/PDF). See any current masthead page for ordering information and Web access instructions.

JA9812047